Geophys. J. Int. (2005) **163,** 727–759 doi: 10.1111/j.1365-246X.2005.02638.x

Apparent polar wander paths for the major continents (200 Ma to the present day): a palaeomagnetic reference frame for global plate tectonic reconstructions

Antonio Schettino[1] and Christopher R. Scotese[2]

[1] *Università degli studi di Camerino, Dipartimento di Scienze della Terra, Via Gentile III da Varano,* 62032 *Camerino (MC), Italy. E-mail: antonio.schettino@unicam.it*

[2] *Department of Geology, University of Texas at Arlington, Arlington, Texas, USA. E-mail: chris@scotese.com*

Accepted 2005 March 11. Received 2005 January 24; in original form 2004 July 12

SUMMARY

Synthetic apparent polar wander (APW) paths for North America, South America, Eurasia, India, Central Africa, Australia and Antarctica for the last 200 Myr are proposed. Computation of these APW paths is based upon the latest version (4.5a) of the Global Paleomagnetic Database (GPMDB), a revised global plate tectonic model since the Early Jurassic, and a new technique for generating smoothed APW paths. The smoothing technique includes the following steps: (1) pre-selection of palaeopoles, including pre-filtering parameters (number of sites, number of samples per site, 95 per cent confidence circle about mean direction, cleaning procedure, and time uncertainty); (2) generation of palaeolatitude and declination plots for a reference site on each continent that combines palaeopoles via a global plate tectonic circuit; (3) independent spline regression analyses of the palaeolatitude and declination plots; (4) removal of palaeolatitude or declination data that deviate by more than 10° from the regression curves (post-filtering process); (5) generation of synthetic APW paths from the resulting palaeolatitude and declination plots. These synthetic APW paths are then rotated into African coordinates to determine the best-fit APW path and a global palaeomagnetic reference frame. Four representative plate tectonic reconstructions and global plate velocity fields are presented for the three time intervals that correspond to globally synchronous changes in plate motion.

Key words: APW (apparent polar wander), Cenozoic, continental drift, Cretaceous, Jurassic, plate tectonics.

1 INTRODUCTION

Plate tectonic reconstructions are based upon hierarchical data structures that describe the relative positions between pairs of plates. Each position of a plate A in the geological past is specified through the Euler pole and angle of a finite rotation that carries this plate from the present position to the position assumed at time *t* relative to a plate B, which is considered at rest with respect to the present geographical frame of reference. Hence, all the rotation poles included in a plate tectonic model are expressed through standard geographical coordinates. However, in these tree-like structures a reference continent occupies the topmost node. The motion of this reference plate must be first determined with respect to an external reference frame. Then, a transformation must be found that translates coordinates relative to the external frame into standard geographical coordinates. The identification of a physically meaningful external reference frame is one of the most interesting fields of research in plate tectonics. In this paper we use palaeomagnetic data to determine the orientation of the root continent with respect to a palaeomagnetic frame of reference. This determination, as well as the translation of the palaeomagnetic coordinates into the corresponding geographical coordinates, requires two basic assumptions.

A first assumption is that the Earth's time-averaged palaeomagnetic field can be modelled through a spherical harmonic expansion having tesseral and sectoral coefficients equal to zero. This geocentric axial hypothesis is justified by the observation that the field is calculated by averaging the data over intervals of time that are supposed to be sufficient to eliminate secular variations. In this instance, the field is symmetric with respect to the spin axis and the magnetic poles will coincide with the geographical poles. This means that we can choose the rotation axis and two arbitrary axes in the equatorial plane as palaeomagnetic reference frame, so that the transformation between palaeomagnetic and geographical coordinates is trivial.

The second assumption is necessary to translate observed inclinations into palaeo-colatitudes, hence to transform inclination–declination pairs into palaeopole positions that determine the orientation of a continent with respect to the palaeomagnetic reference frame. In this paper we will assume as approximately valid the

classic hypothesis that the Earth's magnetic field is produced by a single dipolar source at the centre of the Earth. If we combine this assumption with the previous one, we obtain the well-known geocentric axial dipole (GAD) hypothesis (e.g. Butler 1992).

Apparent polar wander (APW) paths are the usual way to represent the changing orientation of continents relative to the spin axis. Several techniques have been developed during the last two decades for the construction of such curves, but the most widely used is undoubtedly the 'time-averaged, mean pole' method, which uses a sliding-time-window to determine mean poles within disjoint time intervals (e.g. Harrison & Lindh 1982; Besse & Courtillot 1991; Bocharova & Scotese 1993; Van der Voo 1993; Besse & Courtillot 2002). These mean poles are calculated using standard Fisherian statistics, along with the associated precision parameter (K) and cone of confidence (A_{95}).

Besse & Courtillot (1991) first observed that the APW paths from individual plates cannot be independent of one another, as they are related through the plate kinematic model. They therefore combined palaeopoles from different plates to build synthetic APW paths that could be transferred to any desired plate. An obvious advantage of this method is that we can build an APW path for a continent even when only a few reliable data are available for that plate. In this instance, 'foreign' palaeopoles that are rotated into the continent coordinates through the plate kinematic model can make up for the lack of direct information. However, the uncertainty about relative plate positions is the greatest limitation of this technique.

In general, compared with the vector average of palaeomagnetic directions that have been sampled at a single site, the averaging procedure of unit vectors that represent palaeopoles determined at different sites is affected by time uncertainty of individual components, intraplate deformation processes and unknown errors in the rotation model. For instance, Besse & Courtillot (2002) noted that a major source of error was related to local tectonic rotations about the vertical axis. Therefore, one key aspect of the data selection process proposed by these authors was the identification of palaeopoles that were affected by such crustal deformation processes. In these cases they removed the declination data from the data set and used the inclination components only.

If we consider the classic Fisherian statistics of palaeomagnetic directions, the declination and inclination associated with each unit vector are simply angular quantities that determine the orientation of the vectors in a local coordinate system having its origin at the sampling site. In this context the two sets of data cannot be treated separately, as in general the inclination and declination associated with the mean direction will not coincide with the average of all inclinations and the average of all declinations. Conversely, the calculation of a mean palaeopole from a set of palaeopoles that have been determined at different sites does not involve any local coordinate system or information related to the original sampling sites. In this instance the predicted declination at any arbitrary reference point assumes a somewhat different meaning with respect to the usual concept of declination, because it now represents the direction of the palaeopole relative to the selected site in the global frame of reference. Similarly, the concept of inclination is now substituted by the more useful concept of palaeo-colatitude of the reference point, that is by its angular distance from the palaeopole.

As in the case of inclination–declination pairs, the predicted declination and palaeo-colatitude at a reference site are not independent quantities. In fact, the declination associated with the mean palaeopole will not in general coincide with the average of the declinations predicted by each component palaeopole, unless the predicted colatitude is the same for all components. A similar reasoning applies to the palaeo-colatitude. However, if we have arguments to show that the predicted mean declination at a site is wrong, we could try to determine which components cause that deviation. For instance, some palaeopoles could have been sampled on blocks that were subject to vertical axis rotations. These palaeopoles could be removed from the data set in order to obtain a mean palaeopole that furnished the correct value of declination. However, in this instance there is no reason to remove information about palaeo-colatitudes as well. A similar reasoning applies to colatitudes: one or more components could be removed from the data set because secondary geological events (for example, sedimentary inclination shallowing) affected the predicted value of palaeo-colatitude. Also in this case the remaining pieces of information (the declinations) should be retained.

In this paper we propose a filtering technique that is able to remove wrong data while still retaining as much information as possible. This technique is based on the detection of bad palaeopole means through the individuation of anomalous values of the predicted declination or palaeo-colatitude at a reference site. These anomalous values are simply defined as the outliers of a spline regression analysis that is performed on the temporal series of these quantities. The palaeopoles that are responsible for these deviations are then removed from the averaging procedures that generate the corresponding series. This approach implies that two different palaeopole means are calculated at each time, which independently predict the declination and the palaeo-colatitude at the reference site. Then, the predicted values of declination and colatitude are recombined to calculate a representative palaeopole for each time.

In the following sections we present a set of smoothed APW paths and corresponding palaeolatitude and declination plots for seven major continents over the last 200 Myr. These continents are: North America, South America, Eurasia, India, Africa, Australia and Antarctica. The APW paths were calculated using a new technique for computing and smoothing palaeomagnetic pole positions. The palaeomagnetic data used in this analysis are from the latest version (4.5a) of the Global Paleomagnetic Database (GPMDB) (McElhinny & Lock 1990). Compared with previous studies (e.g. Harrison & Lindh 1982; Besse & Courtillot 1988, 1991, 2002; Bocharova & Scotese 1993; Van der Voo 1993), the results presented here are (1) based on a larger data set (9067 available palaeopoles), (2) use a revised global plate tectonic model and (3) take advantage of a new filtering and smoothing technique that produces high-resolution APW paths (one synthetic palaeopole per million years).

Finally, a best-fitting, global APW path will be generated by rotating the synthetic palaeopoles for each of the seven major continents into African coordinates and calculating a mean global pole for each time increment. This best-fitting APW path can be used to define a new set of finite rotations that describes the movement of the reference continent (Africa) with respect to the classic palaeomagnetic reference frame (spin axis). Although a palaeomagnetic Euler pole (PEP) analysis of an early version of our work was presented in Schettino & Scotese (2000), no attempt will be made in this paper to fit small circle tracks to the resulting APW path. We will, however, identify the cusps of the APW path and comment on a possible tectonic interpretation.

In the next section we discuss the global plate tectonic rotation model (plate circuit) that has been used to transfer palaeopoles from one plate to the reference frame of another plate. It is fair to say that the uncertainty in relative plate motions is the greatest limitation of our technique. Then we will describe the smoothing technique and the main features of both the APW paths and palaeolatitude and declination plots. We will show that, based on the shape of

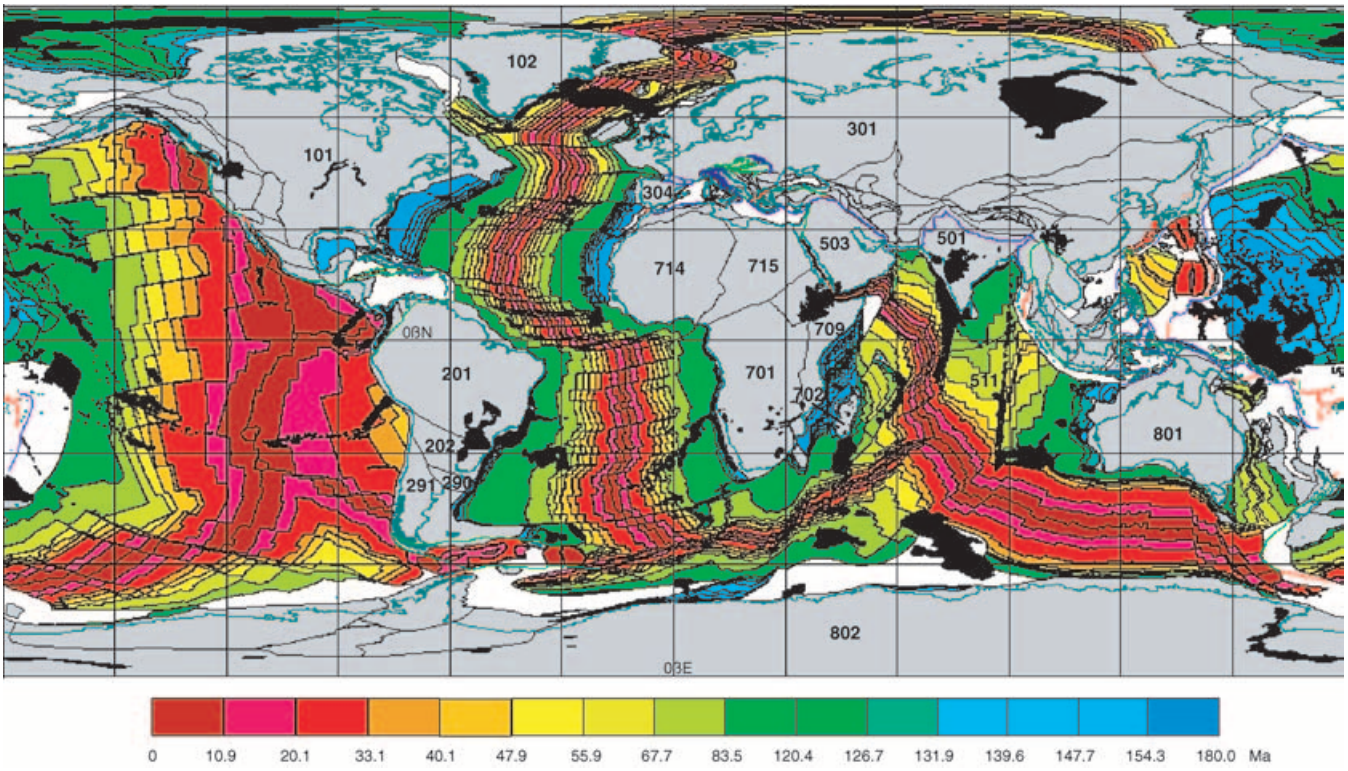

Figure 1. Plate identifiers and outlines of blocks that contribute with palaeopoles to the synthesis of APW paths in the present study. This map also shows the global set of isochrons associated with the rotation model. Colours in oceanic areas represent the age of formation of the corresponding crust, according to the map of Müller *et al.* (1997). Black polygons represent large igneous provinces (LIPs) (Coffin & Eldholm 1994).

the global APW paths, the fragmentation and dispersal of Pangaea since the Early Jurassic can be divided into three main phases: 200–135 Ma, 135–70 Ma and 70 Ma to the recent. Four representative plate tectonic reconstructions and global velocity fields will be presented: M25 (154.3 Ma, Kimmeridgian); M0 (120.4 Ma, Aptian); C34 (83.5 Ma, Santonian–Campanian boundary) and C18 (40.1 Ma, Bartonian). In all our discussions, the geological timescale GTS2004 (Gradstein *et al.* 2004) is used for the correlation between magnetic anomalies and stratigraphic ages.

2 THE GLOBAL PLATE TECTONIC MODEL

As described above, a global APW path can be calculated by rotating palaeopoles from each continent into the reference frame of one continent that is chosen to be the 'reference continent'. In this study, we have chosen Central Africa to be the reference continent. In order to rotate palaeopoles from all the other continents into the African reference frame, an accurate and detailed global plate tectonic model (plate circuit) is required.

The global plate tectonic model described here includes 309 continental tectonic elements mapped by the PALEOMAP Project (Scotese 1990), 2074 features from the Large Igneous Provinces (LIPs) data set (Coffin & Eldholm 1994) and 1031 polygons representing blocks of oceanic crust bounded by transform faults and isochrons. The LIPs data set is a modified version of the digital compilation available via anonymous ftp from the University of Texas Institute for Geophysics, at ftp://ftp.ig.utexas.edu/pub/LIPS. Most of the 1031 elements of oceanic crust were extracted from the latest release (version 1.5) of the digital ocean floor age grid (Müller *et al.* 1997) and the digital compilation of oceanic isochrons of Royer *et al.* (1992) using the method described by Schettino (1999). The remaining oceanic blocks belong to the North Atlantic and Arctic regions and were modelled according to the rotation parameters of Rowley & Lottes (1988).

In this paper we focus on a selected subset of the continental blocks whose relative motions are well constrained by marine magnetic anomalies and fracture zones, or by structural features on land. Only palaeopoles associated with these continental blocks were used. These continental blocks (and the reference numbers that identify them) are: the North American Craton (101), Greenland (102), the Brazilian Craton (201), the Paraná Plate (202), Patagonia (291), Eurasia (301), Iberia (304), India (501), Arabia (503), Central Africa (701), Madagascar (702), Somalia (709), Northwest Africa (714), Northeast Africa (715), Australia (801) and East Antarctica (802). Outlines of these 16 blocks and plates are shown in Fig. 1, along with two other intermediate tectonic elements (511, Central Indian Basin, and 290, Salado Block) which, though they do not directly contribute to the global palaeopole calculations, are kinematically linked to other plates. Fig. 2 shows the global plate circuit that has been used to define relative motions between these plates in this study. The total finite rotations (Euler poles) describing the motions between these plates are given in Table 1.

With the exception of a part of the plate tectonic circuit associated with seafloor spreading in the North Atlantic and Arctic regions, finite rotations for conjugate pairs of major plates were calculated by inversion of the digital ocean floor age grid (Müller *et al.* 1997). Our kinematic solution for the plates bordering the Indian Ocean is slightly different from the solution proposed by Royer *et al.* (1992). We also use a different set of rotation parameters to describe the early

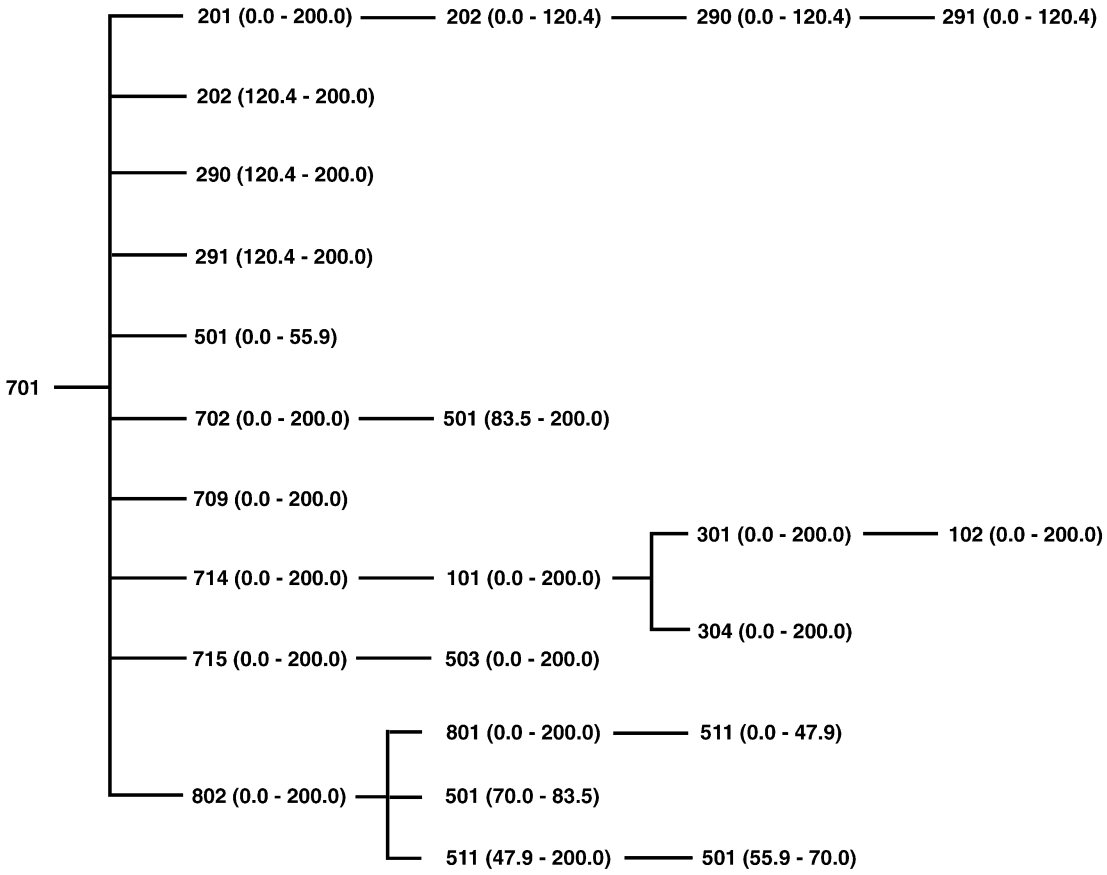

Figure 2. Plate circuit associated with the global rotation model used to combine palaeopoles sampled in different plates: 101, North America; 102, Greenland; 201, Brazilian Craton; 202, Paraná Plate; 290, Salado Block; 291, Patagonia terrane; 301, Eurasia; 304, Iberia; 501, India; 503, Arabia; 511, Central Indian Basin; 701, Central Africa; 702, Madagascar; 709, Somalia; 714, Northwest Africa; 715, Northeast Africa; 801, Australia; 802, Antarctica. Ages are in Ma.

stages of breakup of Gondwana, in particular the relative motion of India and Madagascar prior to the initiation of seafloor spreading in the Mascarene Basin.

The initial fit of Pangaea at 200 Ma (Lower Sinemurian) is shown in Fig. 3 and is based on a revised compilation of the unstretched continent–ocean boundaries (COBs). This compilation combines satellite altimetry data (Sandwell & Smith 1997) and, whenever possible, Moho depth and basement profiles. In particular, the steepest horizontal gradient of gravity anomalies (Blakely 1995) was used to identify the boundaries of unstretched pre-rift COBs. All reconstructions and palaeomagnetic analyses were made using PCME, an interactive software tool for plate tectonic modelling designed by Schettino (1998).

Any accurate reconstruction of the Jurassic and Cretaceous palaeo-continental positions must take into account deformation within Central Africa. Because Africa is the topmost node in the plate circuit, relatively small motions between the African blocks may have large effects on the positions of other continents and may affect the transfer of palaeopoles into African coordinates. This is a good example of the 'tail wagging the dog'. This is an especially worrisome problem for any reconstruction of the Tethyan realm and Mediterranean region, which rely on long plate circuit paths to link the eastern continents of Gondwana (Australia, India and East Antarctica) to Eurasia.

The tectonic setting of Africa is characterized by a high level of magmatic activity and rifting (Sahagian 1988; Wilson & Guiraud 1992; Ebinger & Sleep 1998). Following Genik (1992), we subdivide Africa into five rigid blocks: Northwest Africa, Northeast Africa, Central Africa, Nubia and Somalia. The Cenomanian palaeogeography of North Africa was dominated by the Trans-Saharan Seaway, which extended from the Gulf of Sirte in Libya to the Benue Trough in Nigeria. This seaway resulted from a long period of Early Cretaceous extension, which was pre-dated by Late Jurassic magmatic activity in northeast Brazil and in the Benue Trough. In the Benue Trough, graben formation began in the Aptian (*ca.*117 Ma) (Sahagian 1988), though the onset of this West African Rift System (WARS) occurred in Neocomian time (*ca.*144 Ma) (Guiraud & Maurin 1992). Extension in this region probably ceased in the Santonian (*ca.*85 Ma), when a compressional episode caused folding of the Aptian–Santonian strata (Genik 1992). As we discuss later, the beginning and ending of rifting approximately coincided with two successive cusps on the African APW path (see Fig. 26). This implies that the Cretaceous deformation between the Northwest African Block and the Central African Craton may have been driven by plate tectonic events at global scale.

Our proposed fit of Pangaea at 200 Ma takes into account the pattern of deformation in Africa during the Cretaceous (Wilson & Guiraud 1992; Genik 1992; Guiraud & Maurin 1992) by restoring the North African blocks to their initial orientations with respect to Central Africa. This includes closure of the West African Rift System (WARS) and the restoration of transcurrent motion along the Central African Shear Zone (CASZ) which extended from the Gulf of Guinea to western Sudan. Between 120 and 110 Ma an important phase of strike-slip motion took place between northeast

Table 1. Global rotation model for palaeopole transfer.

Age	Lat.	Lon.	Angle	References
North America–Northwest Africa(101/714)				
3.2	78.81	38.28	0.76	C2A NUVEL-1A; DeMets *et al.* (1994)
10.9	80.07	51.92	2.62	This paper
20.1	79.45	35.46	5.43	This paper
33.1	75.46	1.37	10.03	This paper
40.1	75.29	357.88	12.73	This paper
47.9	75.72	356.32	15.49	This paper
55.9	79.52	359.32	18.03	This paper
67.7	82.58	1.29	21.19	This paper
72.5	81.35	350.85	22.87	Klitgord & Schouten (1986)
74.3	80.76	348.24	23.91	Klitgord & Schouten (1986)
80.2	78.30	341.65	27.06	Klitgord & Schouten (1986)
83.5	76.62	339.49	29.56	This paper
120.4	66.27	340.17	54.45	This paper
126.7	66.10	341.04	56.50	This paper
131.9	65.96	341.50	57.44	This paper
139.6	66.12	341.59	59.90	This paper
147.7	66.53	342.03	62.09	This paper
154.3	67.14	344.02	64.76	This paper
170.0	67.02	346.83	72.10	Klitgord & Schouten (1986)
175.0	66.95	347.98	75.55	Klitgord & Schouten (1986)
200.0	66.95	347.98	75.55	Klitgord & Schouten (1986)
Greenland–Eurasia (102/301)				
10.9	66.43	133.29	2.58	This paper
20.1	68.92	136.60	5.07	This paper
33.1	65.45	137.14	7.39	This paper
40.1	60.07	130.24	8.46	This paper
47.9	53.64	127.19	9.52	This paper
53.3	47.72	125.02	10.39	Rowley & Lottes (1988)
55.9	40.66	125.60	10.71	Rowley & Lottes (1988)
67.6	48.20	125.05	11.95	Rowley & Lottes (1988)
71.6	51.51	123.83	12.40	Rowley & Lottes (1988)
83.5	53.37	121.83	12.93	Rowley & Lottes (1988)
100.0	53.70	120.46	13.60	Rowley & Lottes (1988)
110.0	55.11	120.21	14.33	Rowley & Lottes (1988)
130.0	58.85	122.96	15.39	Rowley & Lottes (1988)
200.0	58.85	122.96	15.39	Rowley & Lottes (1988)
Brazilian Craton–Central Africa (201/701)				
3.2	62.48	320.60	0.99	C2A NUVEL-1A; DeMets *et al.* (1994)
10.9	59.62	321.88	3.65	This paper
20.1	59.63	322.11	7.46	This paper
33.1	57.44	326.02	13.46	This paper
40.1	57.80	327.83	16.53	This paper
47.9	58.79	328.47	19.59	This paper
55.9	61.50	327.50	22.30	This paper
67.7	63.06	326.51	25.38	This paper
83.5	61.77	326.00	33.50	This paper
120.4	50.06	325.42	52.77	This paper
Brazilian Craton–Central Africa (201/701)				
140.0	46.75	327.35	56.40	Martin *et al.* (1981)
200.0	46.75	327.35	56.40	Martin *et al.* (1981)
Paraná Plate–Brazilian Craton (202/201)				
120.4	0.00	0.00	0.00	This paper
Paraná Plate–Central Africa (202/701)				
120.4	50.06	325.42	52.77	This paper
140.0	46.59	327.42	56.95	This paper
200.0	46.59	327.42	56.95	This paper
Salado Block–Paraná Plate (290/202)				
120.4	0.00	0.00	0.00	This paper
Salado Block–Central Africa (290/701)				
120.4	50.06	325.42	52.77	This paper
140.0	44.63	327.48	57.68	This paper
200.0	44.63	327.48	57.68	This paper

Table 1. (*Continued*).

Age	Lat.	Lon.	Angle	References
Patagonia–Salado Block (291/290)				
120.4	0.00	0.00	0.00	This paper
Patagonia–Central Africa (291/701)				
120.4	50.06	325.42	52.77	This paper
140.0	44.61	327.54	58.07	This paper
200.0	44.61	327.54	58.07	This paper
Eurasia–North America (301/101)				
3.2	62.41	135.83	−0.68	C2A NUVEL–1A; DeMets *et al.* (1994)
10.9	65.96	133.73	−2.55	This paper
20.1	68.48	137.01	−5.03	This paper
25.2	66.51	135.11	−5.65	Rowley & Lottes (1988)
33.1	68.76	136.01	−7.69	Rowley & Lottes (1988)
47.9	65.65	139.16	−10.52	Rowley & Lottes (1988)
53.3	62.42	141.02	−12.52	Rowley & Lottes (1988)
55.9	64.17	142.37	−14.08	Rowley & Lottes (1988)
67.6	64.16	146.56	−16.44	Rowley & Lottes (1988)
71.6	65.29	147.22	−17.21	Rowley & Lottes (1988)
83.5	67.66	149.50	−19.52	Rowley & Lottes (1988)
100.0	69.95	149.85	−21.38	Rowley & Lottes (1988)
110.0	71.19	150.07	−22.56	Rowley & Lottes (1988)
130.0	72.77	154.73	−24.34	Rowley & Lottes (1988)
200.0	72.77	154.73	−24.34	Rowley & Lottes (1988)
Iberia–North America (304/101)				
10.9	−67.03	312.88	2.56	This paper
20.1	−68.08	317.13	5.03	This paper
33.1	−51.45	324.03	7.14	This paper
40.1	−64.76	318.13	9.02	This paper
47.9	−72.69	310.87	11.38	This paper
55.9	−73.27	312.81	14.09	This paper
67.7	−74.84	314.38	17.41	This paper
83.5	−87.17	236.60	24.69	This paper
120.4	−71.71	168.36	46.30	Rowley & Lottes (1988)
150.0	−73.59	171.49	52.57	Rowley & Lottes (1988)
200.0	−73.59	171.49	52.57	Rowley & Lottes (1988)
India–Central Africa (501/701)				
3.2	23.57	28.51	−1.32	C2A NUVEL–1A; DeMets *et al.* (1994)
10.9	23.89	32.75	−4.52	This paper
India–Central Africa (501/701)				
20.1	28.89	16.81	−6.92	This paper
33.1	21.01	38.57	−14.60	This paper
40.1	25.24	38.49	−17.11	This paper
47.9	23.89	36.42	−20.32	This paper
55.9	21.48	27.32	−28.90	This paper
India–Central Indian Basin (501/511)				
55.9	−0.90	74.60	6.77	Royer *et al.* (1992)
67.7	−0.40	74.05	6.69	This paper
70.0	1.16	73.19	6.49	This paper
India–Antarctica (501/802)				
70.0	−12.52	187.31	50.63	This paper
80.0	−8.13	191.34	62.08	This paper
83.5	−7.80	190.90	65.10	Royer *et al.* (1992)
India–Madagascar (501/702)				
83.5	−17.54	202.63	55.41	This paper
100.0	−19.96	206.57	58.64	This paper
166.0	−19.96	206.57	58.64	This paper
195.0	−19.16	206.91	60.40	This paper
200.0	−19.16	206.91	60.40	This paper
Arabia–Northeast Africa (503/715)				
4.7	32.75	22.64	−1.89	Le Pichon & Gaulier (1988)
13.0	32.15	22.59	−5.36	Le Pichon & Gaulier (1988)
30.0	32.13	22.58	−6.36	Le Pichon & Gaulier (1988)
200.0	32.13	22.58	−6.36	Le Pichon & Gaulier (1988)

Table 1. (*Continued*).

Age	Lat.	Lon.	Angle	References
Central Indian Basin–Australia (511/801)				
45.0	0.00	0.00	0.00	This paper
47.9	−8.60	169.21	3.74	This paper
Central Indian Basin–Antarctica (511/802)				
47.9	−14.90	206.10	27.70	This paper
55.9	−11.30	200.10	37.70	This paper
67.7	−9.50	193.60	51.60	This paper
83.5	−7.77	190.88	65.10	This paper
200.0	−7.77	190.88	65.10	This paper
Madagascar–Central Africa (702/701)				
115.4	0.00	0.00	0.00	Royer *et al.* (1992)
120.4	5.43	283.04	0.91	This paper
126.7	5.31	283.39	3.21	This paper
131.9	5.40	283.81	4.95	This paper
139.6	5.34	283.57	8.34	This paper
147.7	3.97	288.49	11.33	This paper
154.3	0.29	283.01	13.86	This paper
166.0	0.20	282.81	16.04	This paper
195.0	−2.53	271.35	22.95	This paper
200.0	−2.53	271.35	22.95	This paper
Somalia–Central Africa (709/701)				
3.2	64.26	221.45	−0.20	This paper
4.7	64.26	221.45	−0.29	This paper
30.0	61.18	153.81	−1.10	This paper
200.0	61.18	153.81	−1.10	This paper
Northwest Africa–Northeast Africa (714/715)				
80.2	0.00	0.00	0.00	This paper
Northwest Africa–Northeast Africa (714/715)				
120.4	30.18	9.13	4.15	This paper
200.0	30.18	9.13	4.15	This paper
Northeast Africa–Central Africa (715/701)				
110.0	0.00	0.00	0.00	This paper
120.4	−63.16	124.09	1.50	This paper
200.0	−63.16	124.09	1.50	This paper
Australia–Antarctica (801/802)				
3.2	−13.15	218.25	2.08	C2A NUVEL–1A; DeMets *et al.* (1994)
10.9	−13.20	216.10	6.50	This paper
20.1	−15.40	212.70	12.00	This paper
33.1	−13.90	213.40	20.40	This paper
40.1	−16.50	209.90	23.60	This paper
47.9	−14.10	211.40	24.80	This paper
56.0	−11.80	211.90	25.40	This paper
67.7	−8.70	213.20	25.80	This paper
83.5	−4.90	215.80	26.80	This paper
99.6	−1.50	217.00	27.85	Veevers (1987)
120.4	−4.78	216.21	29.14	Powell *et al.* (1988)
132.5	−6.89	215.70	30.09	Powell *et al.* (1988)
160.0	−8.26	215.37	30.75	Powell *et al.* (1988)
200.0	−8.26	215.37	30.75	Powell *et al.* (1988)

Africa and the Central African Craton along the CASZ (Guiraud & Maurin 1992; Genik 1992). During the Early–Mid Cretaceous, strike-slip and extension between four major African blocks resulted into deformation across the northern and central regions of this plate.

We now address the problem of the fit of the continents that made up eastern Gondwana prior to the initiation of seafloor spreading (approximately Middle Jurassic) in the Mozambique–Riisen–Larsen and Somali basins. We will also discuss the mechanism of separation of India from Madagascar at the Albian–Cenomanian boundary.

Since 1988, several studies have described the tectonic history of the breakup of Gondwana. Scotese *et al.* (1988) presented nine reconstructions (from anomaly M17 to anomaly A2), based on the global isochron map of Larson *et al.* (1985). As pointed out by these

Table 1. (*Continued*).

Age	Lat.	Lon.	Angle	References
Antarctica–Central Africa (802/701)				
3.2	5.57	320.76	0.41	C2A NUVEL–1A; DeMets *et al.* (1994)
10.9	8.25	310.64	1.52	This paper
20.1	10.70	312.10	2.78	Royer & Chang (1991)
33.1	12.00	311.60	5.46	Royer & Chang (1991)
40.1	11.61	315.07	7.03	This paper
47.9	10.26	317.14	8.77	This paper
55.9	5.04	319.96	10.32	This paper
67.7	1.07	318.41	11.84	This paper
83.5	−2.00	320.80	17.85	Royer *et al.* (1988)
120.4	−4.20	330.90	42.80	Royer *et al.* (1992)
126.7	−5.99	332.39	44.86	This paper
131.9	−6.28	332.15	46.60	This paper
139.6	−7.00	333.10	49.71	This paper
147.7	−6.39	331.32	52.63	This paper
154.3	−6.73	330.21	53.93	This paper
166.0	−6.75	329.12	56.11	This paper
195.0	−5.08	321.16	56.86	This paper
200.0	−5.08	321.16	56.86	This paper

authors, the plate tectonic reconstructions showed large overlaps or gaps in the Somali, Mozambique and Antarctic basins at M0 and M17 times. Powell *et al.* (1988) estimated the amount of continental extension that took place between Antarctica and Australia prior to the onset of seafloor spreading (Middle Jurassic, 160 Ma, to the Middle Cretaceous, 96 Ma). Royer *et al.* (1992) published a global isochron chart, which was consistent with plate motions and eliminated most of the inconsistencies from the map of Larson *et al.* (1985). This chart was subsequently used to produce, in conjunction with more recent data, the digital ocean floor age grid (Müller *et al.* 1997). Finally, Roeser *et al.* (1996) presented a detailed, though qualitative, description of the early stages of breakup of the central part of Gondwana based on the analysis of magnetic anomalies in the Mozambique–Riisen–Larsen basins, and these authors suggested that strike-slip motions may have played an important role during the early breakup of Gondwana.

About 180 Ma, during the Middle Jurassic, flood basalts covered much of the Dronning Maud Land region of Antarctica and the Karoo province of South Africa (Brewer *et al.* 1996). In the model of Roeser *et al.* (1996), Africa began to separate from Antarctica and Madagascar at 165 Ma, forming the Mozambique-Riisen-Larsen and Somali-Morondava basins. However, this scenario does not take into account the Tertiary extension along the East African Rift System (EARS). We reconstruct the original position of Somalia with respect to Central Africa by removing about one degree of stretched continental crust across the rift zone, and assign and age of about 175 Ma to the onset of seafloor spreading between eastern Africa and Madagascar/Antarctica.

Regarding the breakup of East Gondwana, an important concern is the amount and direction of strike-slip motion between Madagascar and India prior to the start of seafloor spreading (*ca.*96 Ma). Both Roeser *et al.* (1996) and Royer *et al.* (1992) suggest that a component of transcurrent motion took place along the long, linear coastlines of eastern Madagascar and western India. The model of Roeser *et al.* (1996) requires about 750 km of left-lateral strike-slip motion between chrons M10 and M0. This strike-slip movement links rifting between India and Antarctica with seafloor spreading in the Somali Basin. In contrast, the model of Royer *et al.* (1992) implies 600 km of right-lateral strike-slip movement or transtension between 140 and 100 Ma. This 600 km offset was estimated by

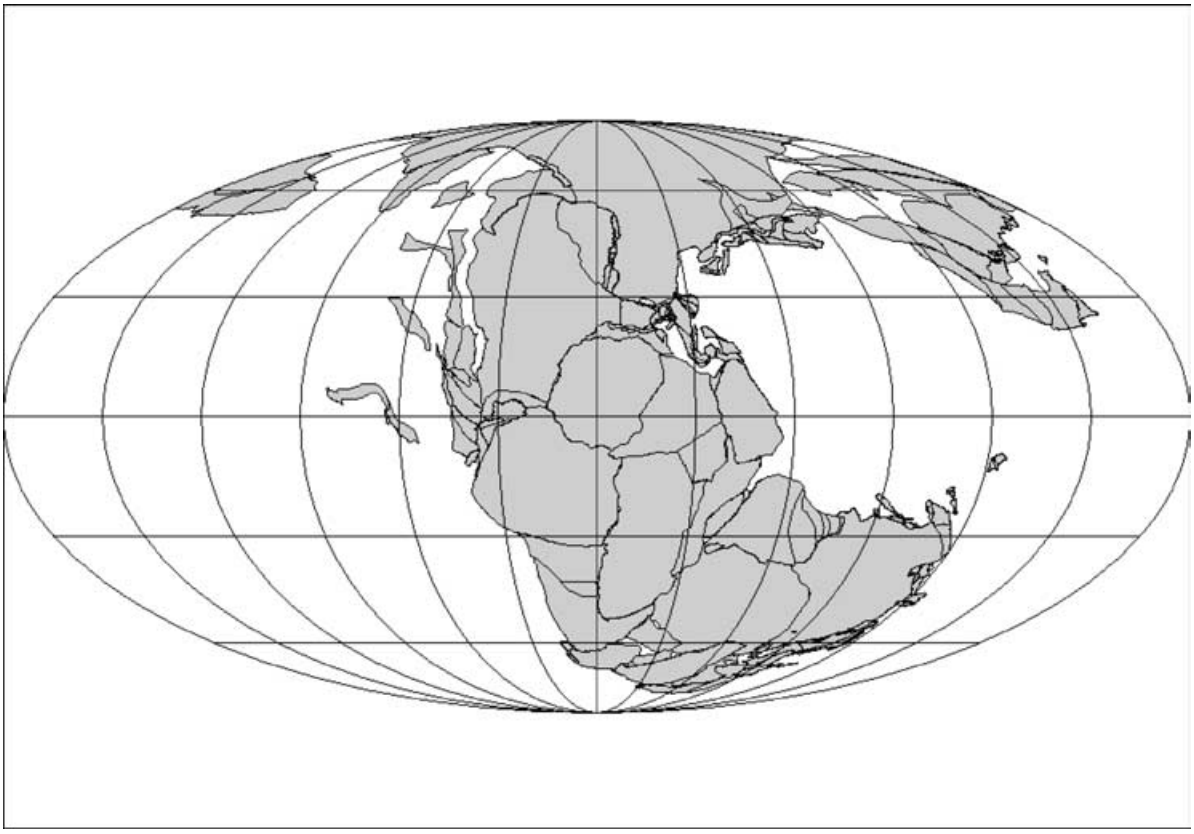

Figure 3. Initial fit of the continents at 200 Ma (Lower Sinemurian).

back-tracking northeast-directed fracture zone flowlines in the Mascarene Basin (e.g. the Mahanoro fracture zone) that offset younger magnetic anomalies (A34–A28). If we start from a fit of the isochrons at anomaly A34 time and move India back along the trend of these fracture zones until India fits against Madagascar, then the southern tip of India will be offset by about 600 km southwards of the southern margin of Madagascar.

The straight continental margins of eastern Madagascar and western India certainly suggest that strike-slip motion might have occurred prior to rifting. However, to date, there is no geological evidence confirming the existence of strike-slip faults (anastomosed arrays of fault zones, flower structures, pull-apart basins, etc.). Consequently, we minimize the amount of strike-slip motion between India and Madagascar, and suggest that, at most, 100 km of left-lateral displacement may have taken place during the Early and Middle Jurassic before the start of active seafloor spreading. This is the minimal amount of displacement required to prevent compression between India and East Antarctica during the early stages of breakup.

With respect to the pre-breakup configuration, our model suggests there was little strike-slip motion between India and Madagascar before the initiation of seafloor spreading in the Mascarene Basin. This in turn implies that the initial stage of separation of India from Madagascar (100 Ma to anomaly 34, 83.5 Ma) occurred along northwest–southeast oriented flow lines of relative motion that were approximately normal to the subsequent northeast–southwest fracture zones (Fig. 4). The main differences between the model presented in this paper and the mechanism proposed by Royer *et al.* (1992) are summarized in Table 2. These differences are expressed in terms of direction and magnitude of the relative velocity field, tectonic regime and total displacement for each stage. Rotation parameters for the fit of India and Madagascar, as well as the other Gondwana continents, are listed in Table 1 and are in substantial agreement with the recent palaeomagnetic-based reconstruction of Torsvik *et al.* (2000).

It is also necessary to briefly discuss the criteria that were used to constrain the fit of the continents on the west side of Africa (North and South Atlantic Oceans). The initial fit of North America to northwest Africa is based on the East Coast magnetic anomaly (ECMA) of eastern North America, the West African coast magnetic anomaly (WACMA) and the match of the continental margins after lithospheric stretching is taken into account (Klitgord & Schouten 1986). The North Atlantic fit, as already mentioned, is based on the reconstructions of Rowley & Lottes (1988) for the North Atlantic and Arctic regions. Regarding the South Atlantic, a tight fit of Patagonia and the Falkland plateau around south-central Africa was obtained by using a new definition of the COB. The COBs were assumed to be coincident with the steepest horizontal gradient of the gravity anomaly field (Blakely 1995) and with tectonic lineations (especially around the Agulhas–Falkland fracture zone), both inferred from satellite altimetry data (Sandwell & Smith 1997). To the north we adopted the fit of Martin *et al.* (1981) between the Brazilian craton and Central Africa, because, when used in conjunction with the fit between Patagonia and southern Africa, it predicts a consistent pattern of deformation in South America.

3 PROCESS OF CONSTRUCTION OF APW PATHS

How best to construct an APW path has been debated by palaeomagnetists for more than two decades. Two very different approaches

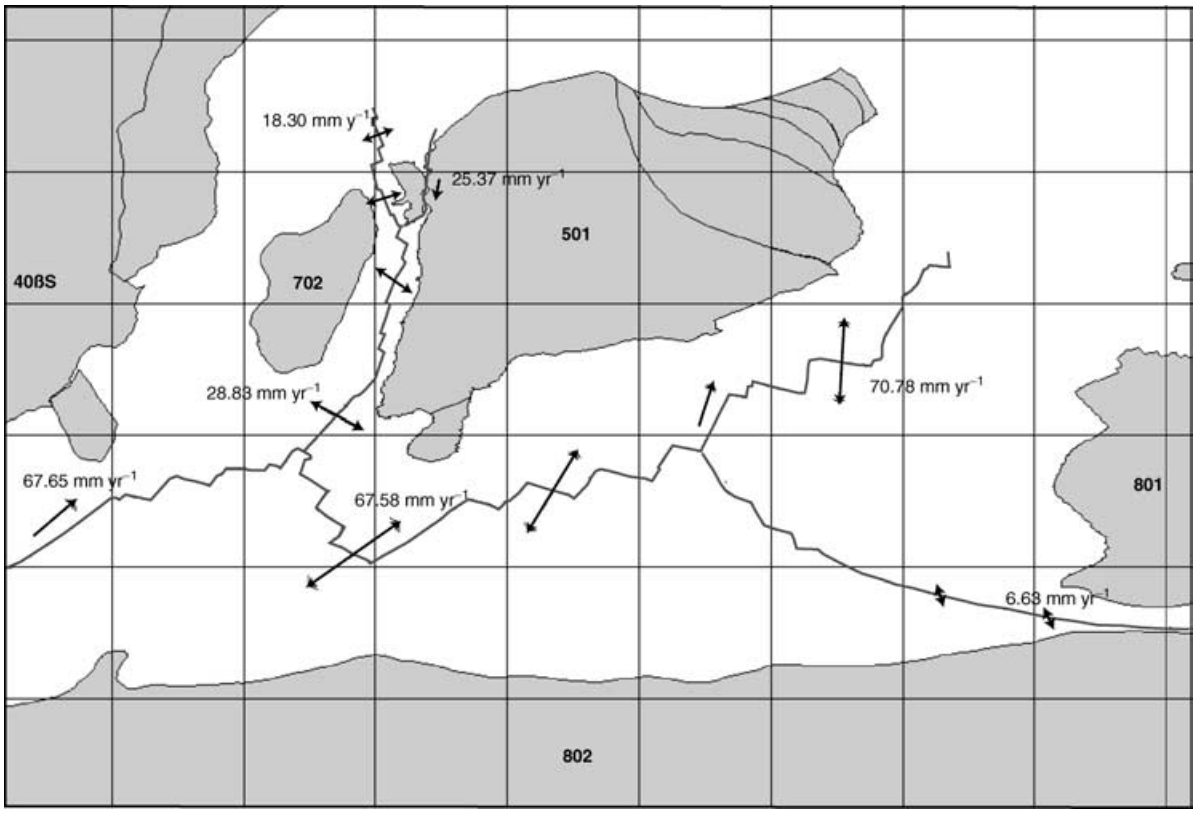

Figure 4. Model for the early stages of separation between India (501), Madagascar (702), Australia (801) and East Antarctica (802). Arrows represent predicted amplitudes and directions of expansion at the spreading centres. This reconstruction refers to chron 34 (83.5 Ma).

Table 2. Comparison between two models for the opening history of the Mascarene Basin.

From (Ma)	To (Ma)	Time (Ma)	Predicted motion India/Madagascar	Tectonic regime	Displacement
Royer et al. (1992)					
83.5	100.0	90.0	27.52 mm yr^{-1} N77E at 39° S	Spreading	—
100.0	115.0	110.0	25.44 mm yr^{-1} N152W at 46° S	High rate of right-lateral strike-slip motion	381 km
115.0	140.0	130.0	9.22 mm yr^{-1} N163W at 46° S	Right lateral transtension	230 km
140.0	166.0	150.0	—	No motion	—
166.0	195.0	170.0	—	No motion	—
This paper					
83.5	100.0	90.0	24.80 mm yr^{-1} N138E at 39° S	Spreading	—
100.0	115.0	110.0	—	No motion	—
115.0	140.0	130.0	—	No motion	—
140.0	166.0	150.0	—	No motion	—
166.0	195.0	170.0	3.61 mm yr^{-1} N51E at 30° S	Low rate of left-lateral strike-slip motion	105 km

have been developed that produce smoothed APW curves from large sets of dispersed palaeopoles.

The first method, which might be called the 'time-averaged, mean pole' method, uses a sliding time-window to calculate mean poles with disjoint time ranges (e.g. Harrison & Lindh 1982; Besse & Courtillot 1991; Bocharova & Scotese 1993; Van der Voo 1993). Each mean pole is calculated using Fisherian statistics, along with the associated precision parameter (K) and cone of confidence (A_{95}). Though the general trend of the APW path is correctly determined using this method, rapid changes in the global plate motions and other important details can be obscured by the averaging procedure. In fact, the minimum duration of each time interval is limited by the local density of available data and by uncertainties in the age of the palaeopoles. From a mathematical point of view, the 'time-averaged, mean pole' method may be considered to be a piecewise linear approximation in spherical coordinates. The curves produced using this method assume a segmented character that may misrepresent the gradual changes that are implicit in the plate tectonic process.

A second technique constructs APW paths by best-fitting smoothed curves through swaths of palaeomagnetic data (APW regression analysis). Parker & Denham (1979) first proposed an interpolation method based on cubic splines. Thompson & Clark (1981) used weighted, least-squares cubic splines to fit smoothed curves to the colatitudes and longitudes of palaeopoles from North America and Europe. Jupp & Kent (1987) developed a sophisticated fitting algorithm based on spherical smoothing splines. However, these authors

did not give proof of convergence and, as a matter of fact, our tests indicate that the algorithm used by Jupp & Kent (1987) does not terminate in certain circumstances. Finally, Musgrave (1989) applied a modified version of the weighted least-squares regression method to a study of Cretaceous and Cenozoic Australian palaeomagnetic data.

In our opinion any regression method, independently of the characteristic of being based on simple or sophisticated statistical techniques, must adequately take into account the physical meaning of palaeomagnetic poles. Consider a compilation of palaeopoles for an arbitrary reference continent A. These data could have been sampled at different sites on the reference plate only or even on different plates. In the latter case, it is assumed that the 'foreign' palaeopoles have been rotated into the reference continent coordinates through a rotation model. The resulting data set consists of a temporal sequence of latitude and longitude pairs (λ_q, φ_q) that determine the orientation of the continent with respect to the palaeomagnetic reference frame through time. If we choose an arbitrary reference site S on this plate, then the sequence can be transformed into a new data set which contains distinct information about the tectonic history of A at site S, consisting of pairs of values that represent the changing values of declination, D, and colatitude, θ, of the reference site through time (Fig. 5). This new representation has several advantages, because it allows us to separate two distinct pieces of information that are included in each palaeopole position relative to S.

As shown in Fig. 5, a first advantage is given by the capability to detect whether the presence of one or more outliers in a group of palaeopoles having the same time t arises from anomalous values of colatitude components, declination components, or both. In the first two cases information associated with individual components can be excluded from the data processing while preserving the remaining piece of information included in the palaeopoles. In fact, in contrast to the classic Fisherian statistics of palaeomagnetic data that have been sampled at a single site, it is now possible that the vector average of unit vectors that come from different sites will be strongly affected by the time uncertainty of individual components, localized intraplate deformation processes and unknown errors in the rotation model. In this instance, the predicted palaeolatitude and/or declination at the reference site would be modified in different ways, according to the relative position of each sampling site with respect to the reference site S. This is illustrated in Fig. 6. Suppose that the mean palaeopole for time t is calculated from the vector average of two palaeopoles $\mathbf{p}$ and $\mathbf{p}'$, the first being sampled at site S and the second one being sampled at site S'. Now suppose that the difference between these two vectors is caused by the fact that S' is located on a crustal block that was subject to local rotation. In this instance, the deformation process would have a small influence on the palaeolatitude component but a significant impact on the estimated declination at site S. If we used both palaeopoles for the construction of an APW path, a tract of the resulting curve would be 'pulled' towards $\mathbf{p}'$ for a time interval centred on t. This implies that the best APW path does not necessarily coincide with the curve on the sphere that approximates at best (in the least-squares sense) the sequence of palaeopole positions through time. In summary, we feel that the extension of Fisherian statistics (that is, the

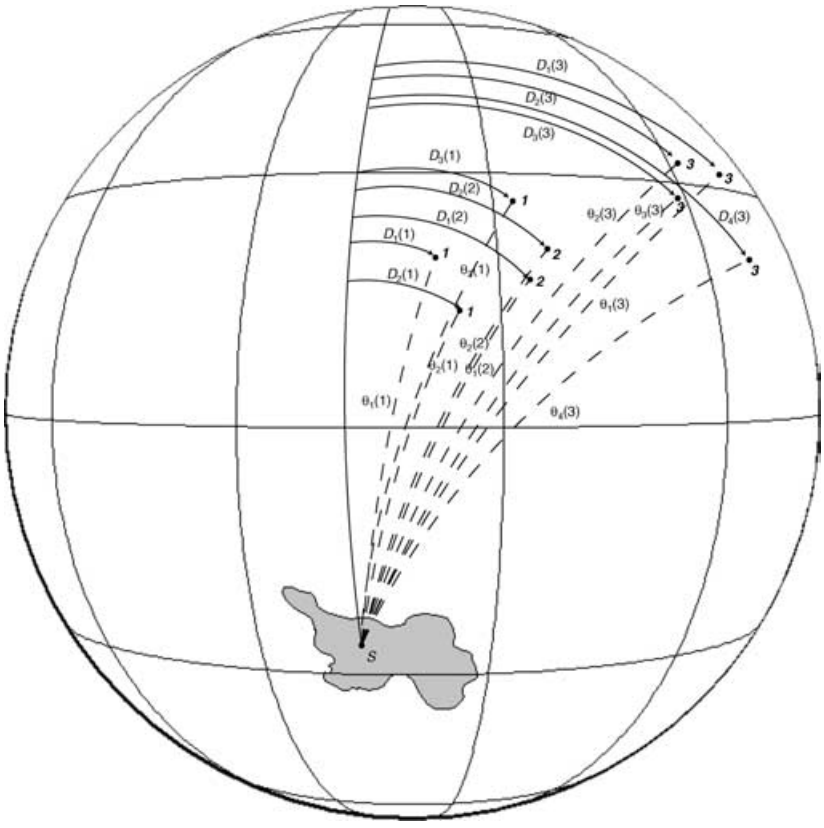

Figure 5. Sketch illustrating the role of declination, D_i, and colatitude, θ_i, components of palaeopoles on the formation of APW paths. In this example three palaeopoles having comparable values of declination relative to a reference site S contribute for time 1, but the third of them has a bad colatitude component. This causes a shift toward the northeast of the mean palaeopole at time 1. Similarly, four palaeopoles having compatible values of the colatitude component contribute to the formation of a mean palaeopole for time 3. However, a bad declination value of the fourth of them determines a shift towards the southeast of the mean at time 3. Projection is a vertical perspective, with meridians and parallels equally spaced by 30°.

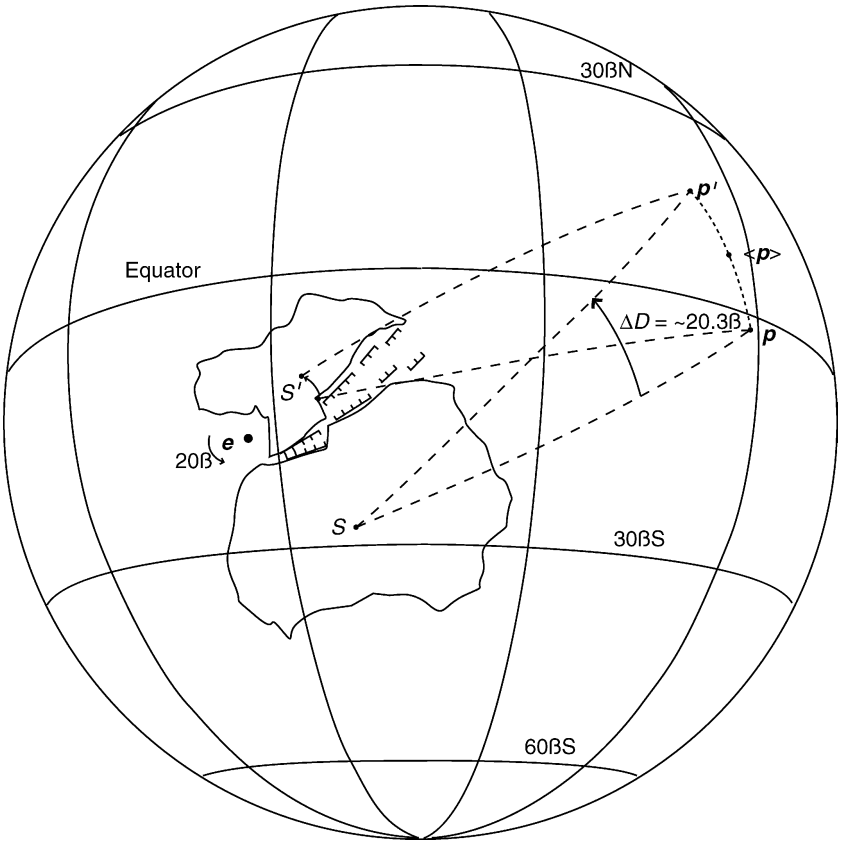

Figure 6. Sketch illustrating the effect of intraplate deformation on the calculation of mean palaeopoles. In this example S' lies on a block that has been rifted from the main plate as a consequence of $\sim 20^\circ$ of rotation about the Euler pole e. This motion causes the palaeopole observed in S' to be shifted to $\mathbf{p}'$. The declination at S calculated through $\mathbf{p}'$ will change by $\sim 20.3^\circ$, and the resulting mean declination associated with $\langle \mathbf{p} \rangle$ would differ significantly from the correct declination D. Conversely, the palaeolatitude of S relative to $\mathbf{p}'$ would differ by only $\sim 4.9^\circ$ with respect to the value relative to $\mathbf{p}$.

vector average of palaeomagnetic directions, or regression methods that are based on palaeopole statistics) to groups of palaeopoles that have been sampled on different sites of the same plate, or even on different plates, does not necessarily produce the best results in the construction of APW paths and therefore it could not give the best representation of the tectonic history of a continent.

A second advantage is related to the fact that the declination, D, and the colatitude, θ, represent kinematic quantities that completely describe the motion of the reference plate with respect to a palaeomagnetic frame. In fact, once we have chosen a reference site on this continent any motion on the sphere can be resolved into three elementary rotations:

(1) A pure north–south component, described by an equatorial Euler pole and associated with variations of latitude of the reference site.

(2) A pure rotation about the vertical axis at the reference site, which is responsible for changes in declination.

(3) A rotation about the spin axis (z axis), which only changes the site longitude.

Fig. 7 illustrates this concept. We also note that the order in which these three elementary rotations are performed does not affect the final result. Finally, though the longitudinal component of the plate motion cannot be resolved through standard palaeomagnetic analysis, this problem does not affect plate tectonic reconstructions. In fact, the palaeomagnetic frame of reference adopted here is built in such a way the z-axis coincides with the spin axis, whereas the choice of x- and y-axes in the equatorial plane is arbitrary. This means that two reference frames, related to one another by a rotation about the z-axis, are equivalent from the point of view of plate tectonics. For instance, we could choose the x-axis in such a way that the reference site always has the same longitude, so that declination D and colatitude θ would completely describe the kinematics of the reference plate. This approach can be found in Besse & Courtillot (1988).

In this paper we propose a new technique for the construction of smoothed APW paths that is not based on the statistics of palaeomagnetic directions. In fact, our approach requires:

(1) The compilation of two series of data for each continent, that is, palaeolatitude λ and declination D of a selected reference point. During this step, palaeopoles $\mathbf{p}_i(t)$ associated with coincident time points are combined into a single mean palaeopole $\mathbf{p}(t)$ by a weighted average with respect to the reciprocal of their 95 per cent confidence cones w_i (that is, the reciprocal of their A_{95} parameter):

$$\mathbf{p}(t) = \frac{\sum \frac{1}{w_i} \mathbf{p}_i(t)}{\sum \frac{1}{w_i}}. \tag{1}$$

Then, standard formulae are applied to the vector $\mathbf{p}(t)$ to estimate the palaeolatitude λ and the declination D at the reference point.

(2) A preliminary regression analysis of these series and the detection of outliers on each curve.

(3) An iterative process for the removal of outliers from the corresponding curves. During this stage a component palaeopole $\mathbf{p}_i(t)$ could be filtered in the process of construction of the smoothed

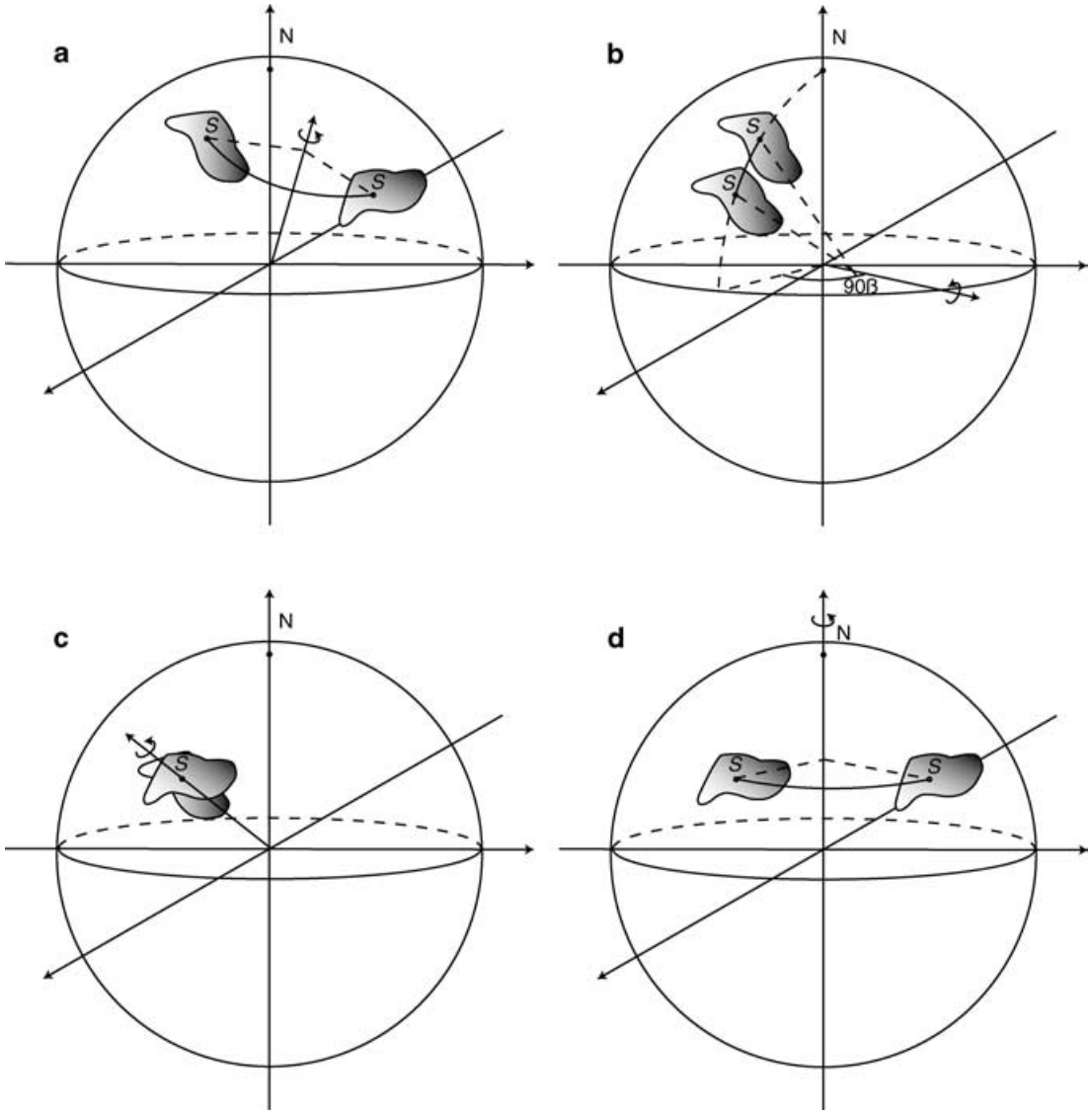

Figure 7. Decomposition of Euler rotations. Given an arbitrary rotation about an Euler pole (a), a reference site *S* will be subject to a variation of latitude, a variation of declination, and a change of longitude. These variations can be described by three elementary transformations: a rotation about an equatorial pole, located 90°E from the initial longitude (b), a vertical axis rotation (c), and a rotation about the spin axis (d).

palaeolatitude curve but it may still participate in the formation of the declination plot, or vice versa. Therefore, two different series of mean palaeopoles were built at the end of this step;

(4) The compilation of an unsmoothed series of mean palaeopoles. Let $(\lambda(t), D(t))$ be the predicted palaeolatitude and declination for time t. If possible, $\lambda(t)$ was calculated from the mean palaeopole $\mathbf{p}_\lambda(t)$ of the palaeolatitude series for time t (eq. 1), whereas $D(t)$ was estimated using the corresponding mean palaeopole $\mathbf{p}_D(t)$ of the declination series. In general these two palaeopoles will not coincide, because the filtering process performed during step 3 removed some (if not all) of the components that were present in the original palaeopole compilation. When either $\mathbf{p}_\lambda(t) = \mathbf{0}$ or $\mathbf{p}_D(t) = \mathbf{0}$ we used the surviving palaeopole to estimate both palaeolatitude and declination at time t. Finally, we used the resulting pairs $(\lambda(t), D(t))$ to calculate representative mean palaeopoles $\mathbf{p}(t)$ for each time t.

(5) Independent regression analyses of the resulting series of values of palaeolatitude, λ, and declination, D. Then, a smoothed series of synthetic palaeopoles, that is, a smoothed APW path was calculated from the resulting smoothed curves of palaeolatitude and declination.

It should be noted that the two temporal series of data used in step 5 (declinations $D_k = D(t_k)$ and palaeolatitudes $\lambda_k = \lambda(t_k)$) have the following basic properties:

(1) They do not contain the same number of elements, because of the application of independent filtering procedures.

(2) The two series are physically independent, because they describe independent components of the plate motion.

(3) Both series have uncertainty on the dependent variable (time t).

(4) The two series are strongly self-correlated, as the values that can be assumed from the variables D and λ (declination and palaeolatitude) at time t are constrained by the values that these variables assume at the preceding time, because accelerations of real plates are limited.

(5) The two regression curves should be characterized by oscillations about the general trend that are compatible with the mean time uncertainty and large-scale periodicity of changes as recorded by the geological history.

Regarding the smoothing technique, we applied non-parametric spline regression analysis to the declination and palaeolatitude time-series. Parametric regression models assume that the form of the regression function μ is known except for a finite number of parameters. Non-parametric regression models, on the other hand, only require some qualitative properties for μ, such that μ belongs to some functional space Γ. A natural measure of smoothness of a curve $\mu = \mu(t)$ is given by

$$\int_a^b \left(\frac{d^m\mu}{dt^m}\right)^2 dt \tag{2}$$

while a standard indicator of goodness of the fit is given by

$$\frac{1}{n}\sum_{i=1}^{n}[x_i - \mu(t_i)]^2 \tag{3}$$

where $x_i = x(t_i)$ are the observed values. Therefore, an overall measure of performance of the estimators could be given by a combination of these two criteria, that is, by minimization of the functional

$$S_q = (1-q)\frac{1}{n}\sum_{i=1}^{n}[x_i - \mu(t_i)]^2 + q\int_a^b \left(\frac{d^m\mu}{dt^m}\right)^2 dt \tag{4}$$

where the parameter $0 < q < 1$ is used as a balancing factor between goodness-of-fit and smoothing of the estimator. If we set $\beta \equiv q/(1-q)$, then the functional to be minimized, S, can be rewritten as:

$$S_\beta = \frac{1}{n}\sum_{i=1}^{n}[x_i - \mu(t_i)]^2 + \beta\int_a^b \left(\frac{d^m\mu}{dt^m}\right)^2 dt. \tag{5}$$

The minimizing function, μ_β, is a natural smoothing spline estimator (Eubank 1988) and the parameter β, which controls balancing between goodness-of-fit and smoothness, is called the smoothing parameter. When β is large ($q \sim 1$) smoothness is favoured, whereas estimators having large mth derivative are penalized. Conversely, small values of β ($q \sim 0$) tend to select classic least-squares estimators and privilege goodness-of-fit. It can be shown that smoothing spline estimators are natural splines, that is, piecewise polynomials subject to a maximum number of continuity constraints. The segmented nature of these functions gives them more flexibility than polynomials and allows a better adaptation to the local characteristics of the data. The parameters β and m can be chosen manually, according to some known properties of the estimator, or computed by algorithms that take into account the actual data and some optimality criteria. When the only assumption about μ is that this function is continuously differentiable and has a square integrable second derivative, then $m = 2$ and the resulting estimator is a cubic smoothing spline.

We used natural cubic smoothing splines in our analysis ($m = 2$), whereas the smoothing parameter β was chosen independently for each curve, as will be discussed in the next section.

4 PALAEOMAGNETIC ANALYSIS

We have seen in the previous section that the declination, D, and the palaeo-colatitude, θ, are site-dependent palaeomagnetic variables that can be calculated from known palaeopole positions. In general, any palaeopole may be used to calculate palaeolatitude and declination at an arbitrary site on the same plate or even on another plate (when the relative positions of the two continents are known).

Our method is a spline-based regression analysis that fits smoothed curves through plots of declination and palaeolatitude. The palaeomagnetic data for this analysis is from the GPMDB (version 4.5a; McElhinny & Lock 1990), which includes 9067 palaeopoles for all ages published from 1949 to 2003 June. This version has been recently updated using the latest stratigraphic chart published by the International Commission on Stratigraphy (Gradstein *et al.* 2004). We have added a table to the GPMDB, the PLATES table, that lists the tectonic elements (continents, terranes, blocks, etc.) that comprise our global plate tectonic model (Schettino & Scotese 2001). Each palaeopole in the modified version of the GPMDB is given an additional attribute, a tectonic element number, that identifies the continent, terrane or fault-bounded block where the palaeomagnetic data were sampled. The plate identifier attribute is the link between the PMAGRESULT table and the PLATES table. Palaeopoles were assigned to tectonic elements according to the sampling site using a spherical point-in-polygon algorithm developed by Schettino (1999).

In this analysis, we selected 1376 palaeopoles from the GPMDB that had a mean magnetization age between 0 and 200 Ma, and that belonged to the North American Craton (101), Greenland (102), the Brazilian Craton (201), the Paraná Plate (202), Patagonia (291), Eurasia (301), Iberia (304), India (501), Arabia (503), Central Africa (701), Madagascar (702), Somalia (709), Northwest Africa (714), Northeast Africa (715), Australia (801) and East Antarctica (802). A non-restrictive pre-filtering procedure was applied to this subset, in order to select palaeopoles that matched the following palaeomagnetic reliability criteria: $B \geq 4$ (number of sites), $N/B \geq 4$ (mean number of samples per site), ED95 $\leq 15^\circ$ (95 per cent confidence interval), DEMAGCODE ≥ 2 (cleaning procedure code) and $\Delta t \leq 20$ Ma (half-interval of age uncertainty). An 'age' was assigned to each palaeopole by taking the mean primary or (in some cases) secondary magnetization age, as defined by the fields LOMAGAGE and HIMAGAGE of the PMAGRESULT table. Superseded palaeopoles and data already included in other results were excluded from subsequent calculations. We believe that these filtering parameters eliminated the most unreliable palaeomagnetic results, while leaving a sufficient number of palaeopoles to calculate meaningful estimates of error. The 442 palaeopoles that passed the selection criteria are listed in Table 3 (available in the online version of this article).

In the next step, all 442 palaeopoles were rotated in turn to North American, South American (Brazilian Craton), Eurasian, Indian, Central African, Australian and Antarctic coordinates, according to the global plate tectonic rotation model (Table 1). At this stage, palaeopoles having the same mean magnetization age were averaged to obtain mean poles for each 1 Myr time interval. We used these mean palaeopoles to construct preliminary palaeolatitude and declination plots for each of the seven continents. In order to construct the declination (D) and palaeolatitude (λ) plots, reference sites (λ_s, φ_s) near the centre of each continent were chosen. The location of these reference sites are listed in Table 4. A preliminary smoothed curve was fitted through the declination and palaeolatitude plots using non-parametric spline regression analysis.

Spline curves generated during the previous step showed that some palaeolatitude or declination values, calculated from mean palaeopoles, deviated from the preliminary regression model of palaeolatitude or declination by more than 10°, 20° or even 30°. A post-filtering process was then employed that removed those outliers that caused the observed deviations. This analysis was performed independently for each continent and for each curve (palaeolatitude or declination).

Table 4. Parameters used in regression analysis and resulting standard regressions errors.

Plate	Name	λ_s	φ_s	β_λ	β_D	δ_λ	δ_D	n_λ	n_D
101	North America	55°N	270°E	300	30	4.31	4.67	408	334
201	South America	10°S	300°E	100	50	4.22	4.49	411	389
301	Eurasia	60°N	75°E	50	100	4.65	5.30	398	342
501	India	24°N	77°E	100	100	4.65	4.18	400	377
701	Central Africa	0°N	25°E	200	100	4.67	4.45	396	400
801	Australia	22°S	134°E	100	100	4.31	4.93	399	375
802	Antarctica	80°S	85°E	100	100	4.49	4.37	413	233

n_λ and n_D are respectively the total number of palaeopoles used in regression analysis of palaeolatitude and declination after the post-filtering process; β_D and β_λ are respectively the smoothing parameters used for the regression analysis of declination and palaeolatitude plots; λ_s is the present latitude of the reference site, whereas φ_s is the longitude; δ_λ and δ_D are the rms errors of residuals for the smoothed palaeolatitude and declination curves.

As explained in the previous section, we did not completely remove palaeopoles from the data set, unless they caused deviations in all 14 plots. In other words, a single component could contribute to palaeolatitude or declination curves for one continent but could be excluded from similar computations for other continents. The reason for this is that even a high-quality palaeopole, when transferred from one plate to another, might be unusable due to systematic errors in declination or colatitude. In general, the applicability of the palaeopole transfer method (via the global plate tectonic rotation model) depends on the relative positions of the plates at the time of the reconstruction and the nature of the palaeolatitude and declination errors.

In order to correct for potential declination and palaeolatitude errors, we applied the post-filtering procedure described above to each of the 14 declination and palaeolatitude curves. Table 3 indicates which palaeopoles were removed, and whether the palaeopoles were removed because of declination errors or palaeolatitude errors. A quality factor, Θ, has been given that measures the 'transferability' of each palaeopole. A quality factor $\Theta = 1.0$ indicates that the palaeopole was used on all of the 14 curves. A quality factor $\Theta = 0.0$ indicates that the palaeopole was never used. Intermediate values of Θ indicate partial usage. The removal was performed in successive steps, starting with the most deviating components, until the mean palaeopoles produced palaeolatitudes or declinations that deviated by less than 10° from the preliminary spline regression curves. At each step, new temporary regression plots were calculated using the partially filtered set of palaeopoles. Furthermore, some palaeopoles were removed to adjust the following boundary conditions within 1°:

$$\begin{aligned} &\lambda(t) \rightarrow \lambda_s \qquad \text{for } t \rightarrow 0 \\ &D(t) \rightarrow 0 \qquad \text{for } t \rightarrow 0. \end{aligned} \tag{6}$$

Application of eq. (6) was necessary for consistency with the geocentric axial dipole (GAD) hypothesis (e.g. Butler 1992) along the whole time interval from 200 Ma up to the present. In fact, palaeopole locations (λ_q, φ_q) that were used in the computation described above are those listed in the GPMDB (PMAGRESULT table), which were calculated from declination and inclination values using the well-known dipole formula. This means that the results presented in this paper are valid within the limits of the GAD approximation. An estimation of the magnitude of this approximation can be given, in terms of Gauss expansion coefficients, by the ratios of the zonal coefficients g_2^0 (quadrupole) and g_3^0 (octupole) with respect to the dipolar term g_1^0, granted that the non-zonal coefficients of the time-averaged palaeomagnetic field can be considered as negligible.

Livermore *et al.* (1983, 1984) found the following interesting results: $g_2^0/g_1^0 = 0.05$ for the last 35 Myr; $g_3^0/g_1^0 = 0.02$ for the last 5 Myr; finally $|g_2^0/g_1^0| \leq 0.1$ during the period between 200 and 35 Ma. In a more recent study, performed on marine magnetic anomalies, Acton *et al.* (1996) estimated that the quadrupole component was about 6 per cent of the size of the dipole component during the Brunhes normal polarity chron (0.78–Recent). Finally, a comprehensive study of McElhinny *et al.* (1996) confirmed that $g_2^0/g_1^0 \cong 0.05$ for the last 5 Myr. It is easy to calculate that a large quadrupole term $g_2^0/g_1^0 = 0.1$ cannot cause more than 5° of deviation in the site palaeolatitudes, whereas a large octupole term $g_3^0/g_1^0 = 0.1$ will determine up to 7.5° of deviation.

In summary, a geocentric axial dipolar palaeomagnetic field is assumed for the considered time range (200–0 Ma). Consequently even for the top of this interval (the recent past) we assume that the time-averaged palaeomagnetic field can be modelled according to the GAD hypothesis. Therefore, site palaeolatitudes must tend to coincide with the present-day latitudes, and declinations must tend to be zero. In other words, no far-sided (Wilson 1970) or right-handed effects (Wilson 1972) must be included in the resulting APW paths because these features are related to higher-order coefficients of the spherical harmonic expansion. We note that calculations performed without the boundary condition (6) led to the far-sided effect for the recent past.

The previous analysis was successful for all continents. Table 4 reports the parameters that were adopted in the post-filtering process and the non-parametric spline regression analysis of palaeolatitude and declination temporal series.

Palaeomagnetic data were equally weighted, because a rigorous application of weighting criteria would have to take into account time uncertainty—a problem that cannot be addressed within the scope of this study. The smoothing parameters β_λ and β_D were chosen independently for each series by visual inspection of the regression curves, such that the rms error of residuals, δ_D and δ_λ, were approximately equal (Table 4) and high-frequency components related to the noise were removed. One palaeopole, result 7902, was considered to have reversed polarity (and the corresponding coordinates appear to be inverted in Table 3). The resulting statistics of residuals for each continent are shown in Figs 8–14. (Figs 8–14 can be seen in the online version of this article only.) We note that in most cases the distribution of residuals is not Gaussian, though all curves have a low skewness. This is a consequence of the post-filtering procedure and the arbitrary manual selection of the smoothing parameters β_λ and β_D. In fact, these quantities could be chosen automatically by an algorithm that searched for the best match between the effective distribution of the residuals and the theoretical normal distribution having the same mean and standard deviation.

We did not apply automatic selection of smoothing parameters for the reasons explained above. The declination and palaeolatitude of a reference site are kinematic quantities that represent the plate motion. Hence, the general trend of the corresponding curves must match both physical and geological constraints. Physical constraints are represented by the request that the expected values of velocity and acceleration at any time be compatible with plate dynamics, whereas geological constraints are given by the stratigraphic record on a global scale. Finally, the regression curves must not be characterized by oscillations about the general trend having frequency comparable with the mean time uncertainty of the palaeomagnetic data.

Tables 5–11 report, for each continent, the results of the post-filtering process and spline regression analysis. (Tables 5–11 are available in the online version of this article only.) In these tables, pairs (λ_q, φ_q) represent mean palaeopole positions, calculated from estimated palaeolatitudes λ and declinations D at the reference sites (λ_s, φ_s). Similarly, the spline regression values of palaeolatitude ($\langle\lambda\rangle$) and declination ($\langle D\rangle$) were combined to produce synthetic palaeopole locations ($\langle\lambda_q\rangle, \langle\varphi_q\rangle$) for each plate. The predicted 95 per cent confidence cones (A_{95}) of palaeopole means ($\boldsymbol{p}_\lambda(t)$ or $\mathbf{p}_D(t)$) (eq. 1) were computed with the following formula:

$$w = \frac{1}{\sum \frac{1}{w_i}}. \tag{7}$$

Then, declination and palaeolatitude uncertainties were estimated as follows:

$$\delta D = \operatorname{asin}\left(\frac{\sin w}{\sin\theta}\right) \tag{8}$$

$$\delta\lambda = \frac{1}{2} w(1 + 3\cos^2\theta) \tag{9}$$

where $\theta \equiv \pi/2 - \lambda$ is the palaeo-colatitude. These uncertainties were used in turn for calculating the 95 per cent confidence cones (A_{95}) of the representative palaeopoles $\mathbf{p}(t) \equiv (\lambda_q, \varphi_q)$ listed in Tables 5–11.

In summary, we calculate palaeopole means ($\mathbf{p}_\lambda(t)$ or $\mathbf{p}_D(t)$) and associated A_{95} for each time t of the palaeolatitude or declination series using eqs (1) and (7). Once the post-filtering process is terminated, we use palaeopole positions $\mathbf{p}_D(t)$ and $\mathbf{p}_\lambda(t)$ for calculating respectively declination $D(t)$ and palaeolatitude $\lambda(t)$ at the reference site. The corresponding uncertainties are estimated using eqs (8) and (9). Finally, a representative palaeopole $\mathbf{p}(t) \equiv (\lambda_q, \varphi_q)$ for each time t is determined by recombining the predicted palaeolatitude and declination ($\lambda(t)$, $D(t)$) at the reference site for time t. It should also be noted that the smoothed APW paths resulting from the recombination of spline regression values of palaeolatitude ($\langle\lambda\rangle$) and declination ($\langle D\rangle$) are completely independent of the choice of reference sites in each plate.

5 RESULTS: DECLINATION AND PALAEOLATITUDE CURVES AND SYNTHETIC APW PATHS

Figs 15–21 show the palaeolatitude and declination curves that result from the regression and post-filtering analysis described in the previous section. Figs 22–28 are synthetic APW paths that were constructed using the declination and palaeolatitude values from the smoothed regression curves. These APW paths were calculated using palaeolatitudes and declinations estimated from the smoothed regression plots (Figs 15–21). Tables 5–11 list present-day coordinates (latitude, longitude) of the palaeopoles that make up each APW path.

In this section we discuss the results of the analysis, paying particular attention to the shapes of the regression curves and their implications with regard to plate motion and times of global plate reorganization. The tectonic history of each continent will be separated into distinct phases on the basis of synchronous changes in the palaeolatitude and declination trends, and/or the presence of special features (e.g. loops, hairpins) in the corresponding APW paths.

5.1 North America

Palaeolatitude and declination plots for North America (Figs 15a and b) show that the centre of the North American Plate (southwest Hudson Bay, 55°N, 270°E) was subject to ∼28° of clockwise rotation between 200 and 138 Ma. During the same period, this point on North America migrated northwards by ∼23°, at a mean velocity of ∼40.6 km Myr^{-1}. The palaeolatitude of north-central North America remained approximately constant between 138 Ma and the present. However, three additional rotations are observed in the declination plot: counter-clockwise between 138 and 102 Ma, clockwise between 102 and 73 Ma and strongly counter-clockwise between 73 Ma and the present day. About 25° of counter-clockwise rotation of north-central North America has occurred during the last 73 Myr.

Four phases are also evident in the corresponding APW path (Fig. 22). The 138 Ma transition is marked by a change of direction and slowing down of polar wandering. The 102 Ma phase boundary is associated with the apex of a narrow hairpin that characterizes the period between 120 and 80 Ma. Finally, the 73 Ma transition is visible as a cusp in the APW curve and the starting point of the accelerated wandering path that encompasses the Late Cretaceous and the Cenozoic.

The North American APW path shows few secondary differences with respect to the curve found by Besse & Courtillot (2002). These differences are mainly represented by the Miocene tract and by the lack of the characteristic loop detected by Besse & Courtillot (2002) between 50 and 110 Ma. Conversely, the curve illustrated in Fig. 22 differs significantly from Jurassic and Cretaceous APW paths that include palaeopoles from the Colorado Plateau (e.g. Ekstrand & Butler 1989; Bazard & Butler 1994).

5.2 South America

Figs 16(a) and (b) illustrates the changing palaeolatitude and rotation of the Brazilian Craton during the last 200 Myr. Between 200 and 137 Ma we observe clockwise rotation (∼17°) and northward movement of the reference site (western Brazil, 10°S, 300°E). The total northward displacement was about ∼15°, (∼1668 km) at a rate of ∼26 km Myr^{-1}. During the next phase, between 137 and 74 Ma, South America did not rotate significantly but moved ∼13° southwards. From 74 to 48 Ma the continent slowly moved southwards by ∼1.5°. Finally, during the last phase (48 Ma–present day), South America was subject to 7.5° of northward displacement and no rotation.

The smoothed APW path of South America is illustrated in Fig. 23. The portion of the APW path between 150 and 120 Ma is represented by a narrow loop having the apex at 137 Ma. Similarly, the portion between 100 Ma and the present day is represented by a prominent U-shaped bend.

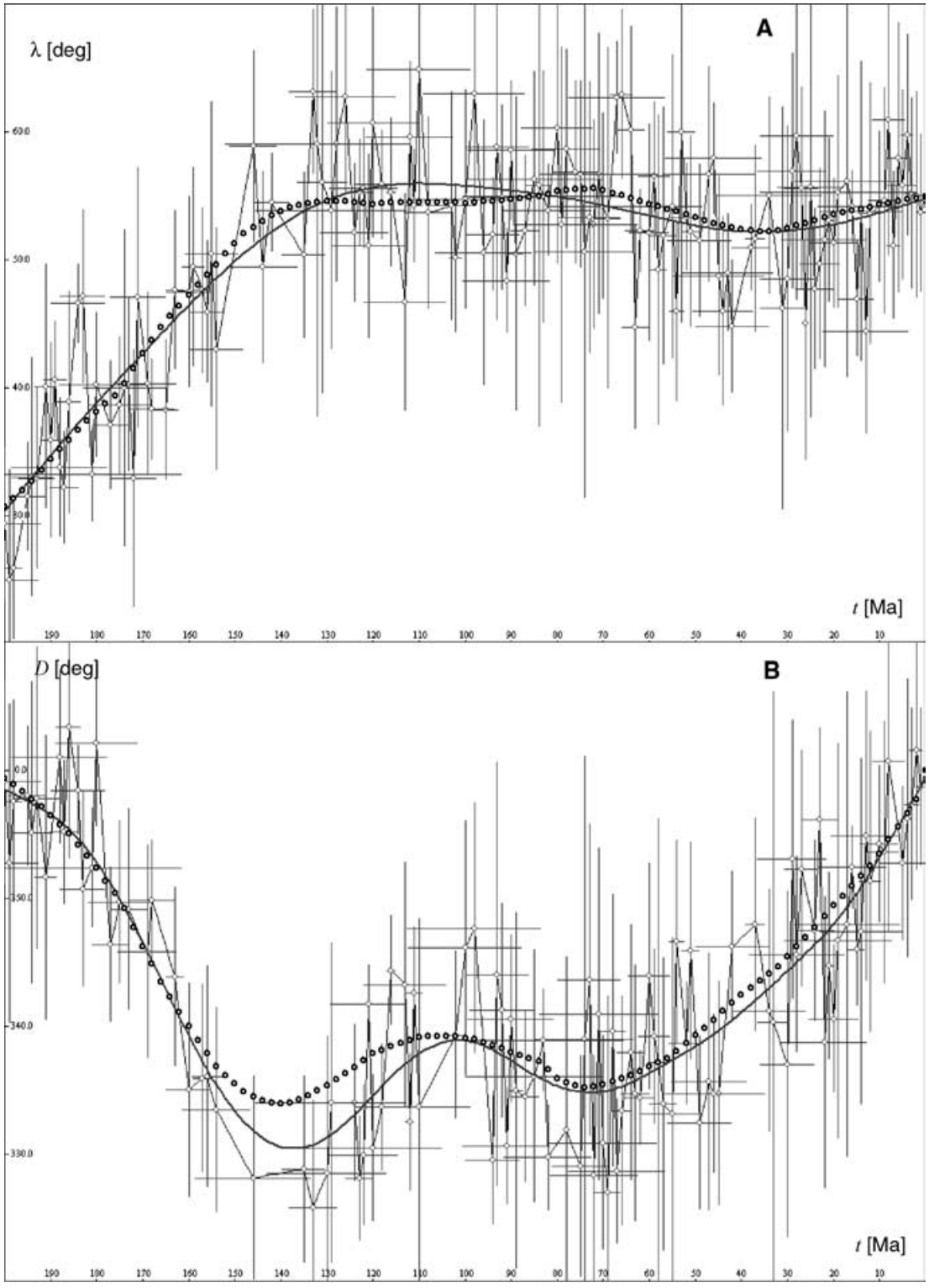

Figure 15. (A) Palaeolatitudes and (B) declinations of a reference point in North America at 55°N, 270°E (thin circles with error bars). Solid lines represent spline regression curves with smoothing parameters $\beta_\lambda = 300$; $\beta_D = 30$. Circles: model-predicted palaeolatitudes (A) and declinations (B).

5.3 Eurasia

Palaeolatitude and declination plots for Central Eurasia (West Siberian lowlands, 60°N, 75°E) are shown in Figs 17(a) and (b). These curves can be divided into three distinct phases. During the first phase (200–135 Ma) the palaeolatitude of central Eurasia fell from 73°N to 54°N. A clockwise rotation of ∼50° accompanied this southward movement. The next period (from 135 to 72 Ma) was characterized by little or no systematic change in palaeolatitude or declination. The last phase, which encompasses the entire Cenozoic,

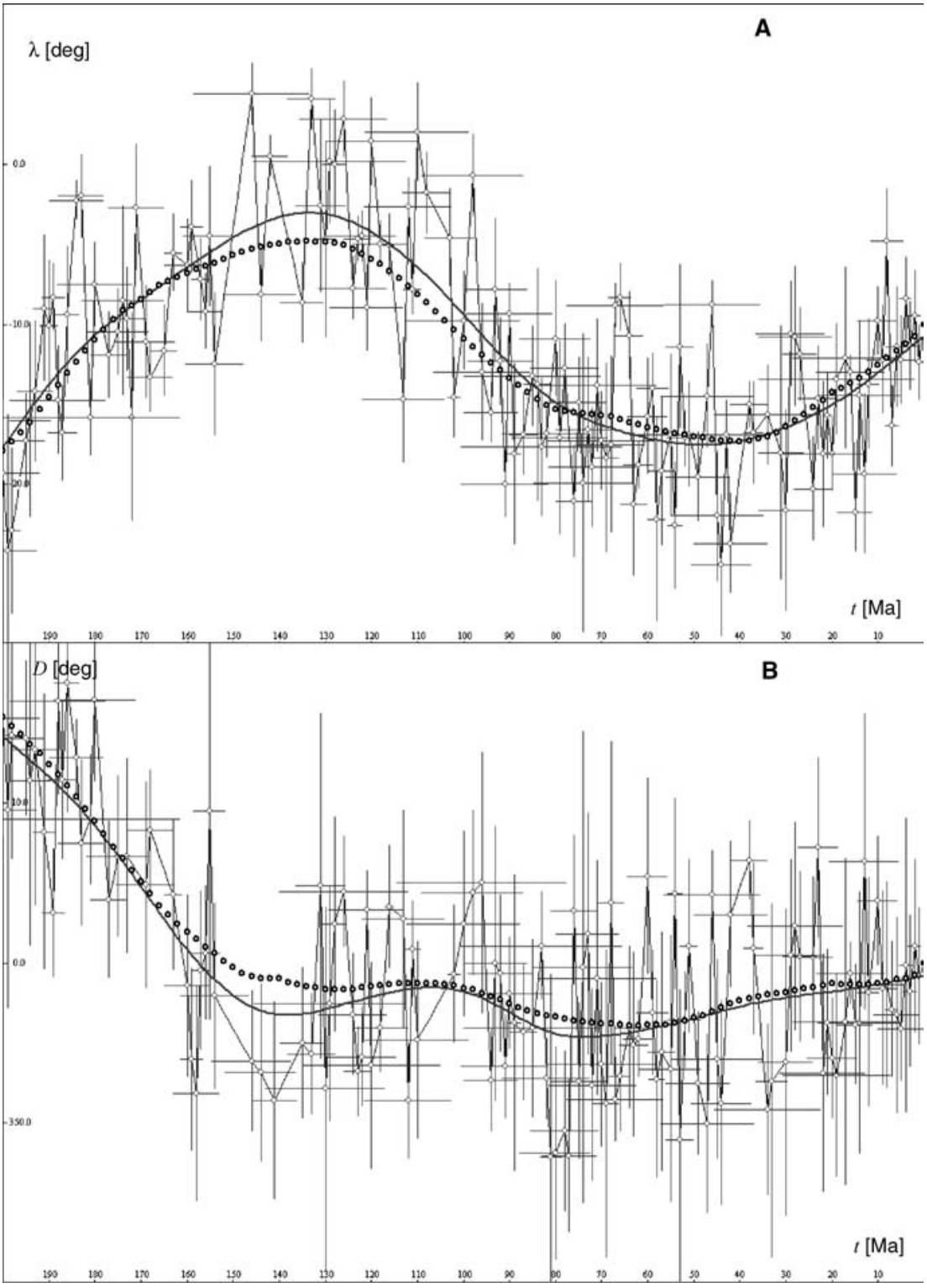

Figure 16. (A) Palaeolatitudes and (B) declinations of a reference point in South America at 10°S, 300°E (thin circles with error bars). Solid lines represent spline regression curves with smoothing parameters $\beta_\lambda = 100$; $\beta_D = 50$. Circles: model-predicted palaeolatitudes (A) and declinations (B).

combines the slow northward movement of Central Eurasia with a 20° clockwise rotation.

A long standstill between 110 and 70 Ma is the most prominent feature of the APW path for Eurasia (Fig. 24). The Jurassic and the Cenozoic tracts of this path make a right-angle bend emerging from the Cretaceous standstill.

5.4 India

The palaeolatitude and declination plots for India (reference site at 24°N, 77°E) are shown in Figs 18(a) and (b). Only two phases of movement and rotation are easily identified, on the basis of events that occurred between 140 and 120 Ma. At 140 Ma

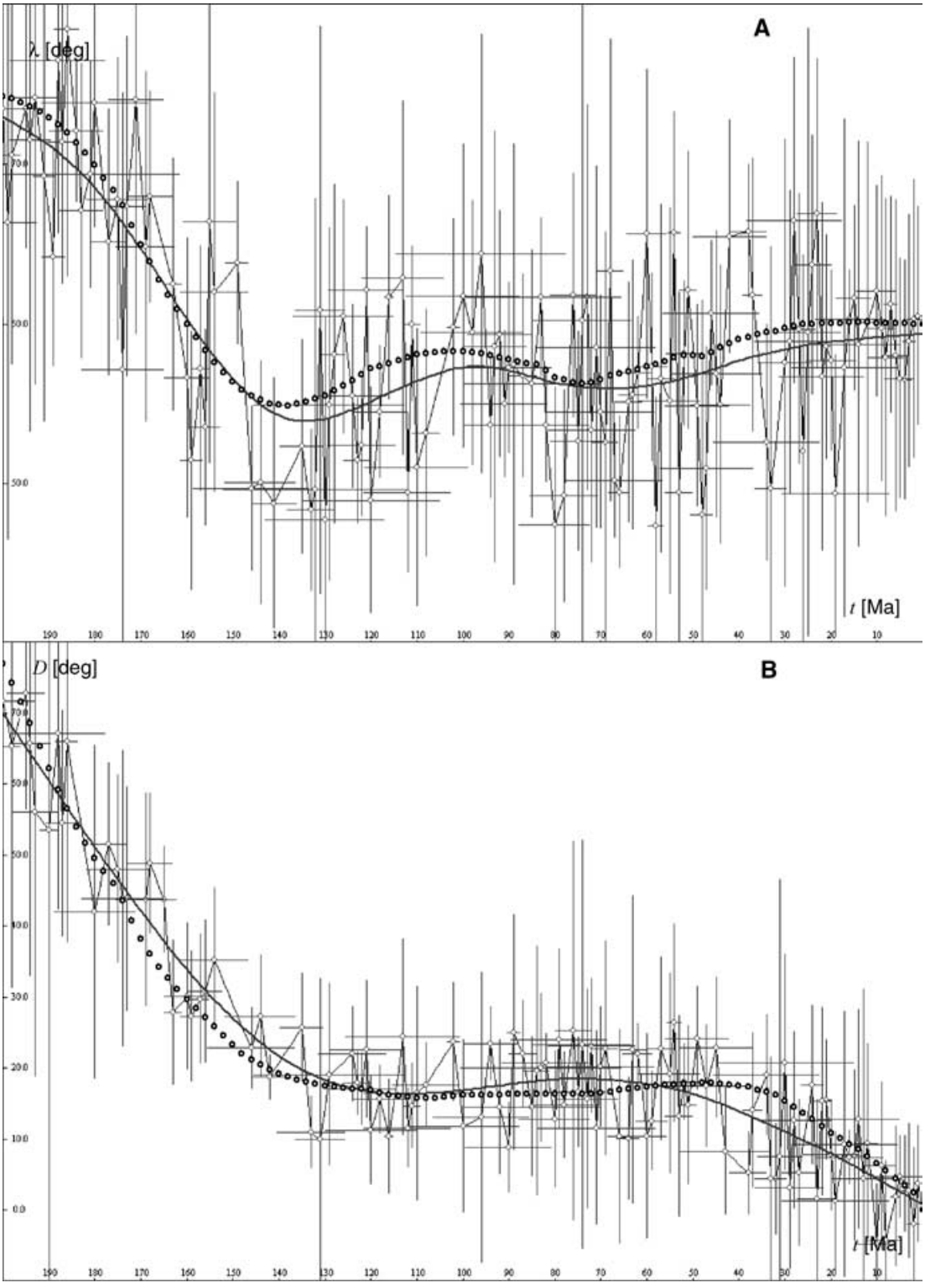

Figure 17. (A) Palaeolatitudes and (B) declinations of a reference point in Eurasia at 60°N,75°E (thin circles with error bars). Solid lines represent spline regression curves with smoothing parameters $\beta_\lambda = 50$; $\beta_D = 100$. Circles: model-predicted palaeolatitudes (A) and declinations (B).

Central India ceased its slow clockwise rotation and started to rotate counter-clockwise. This rotation continued for the whole Cretaceous and Cenozoic. Regarding the palaeolatitude of the reference site, we observe that a transition occurred some time later, at 120 Ma, when India started its rapid northward motion. During the Late Cretaceous and Early Cenozoic, India travelled 5200 km northwards and rotated ∼55° counter-clockwise, eventually colliding with Asia during the Late Lutetian–Early Bartonian. At about 40 Ma, both the rate of northward motion and the rate of rotation slowed. During this last phase of motion, India has driven ∼2100 km

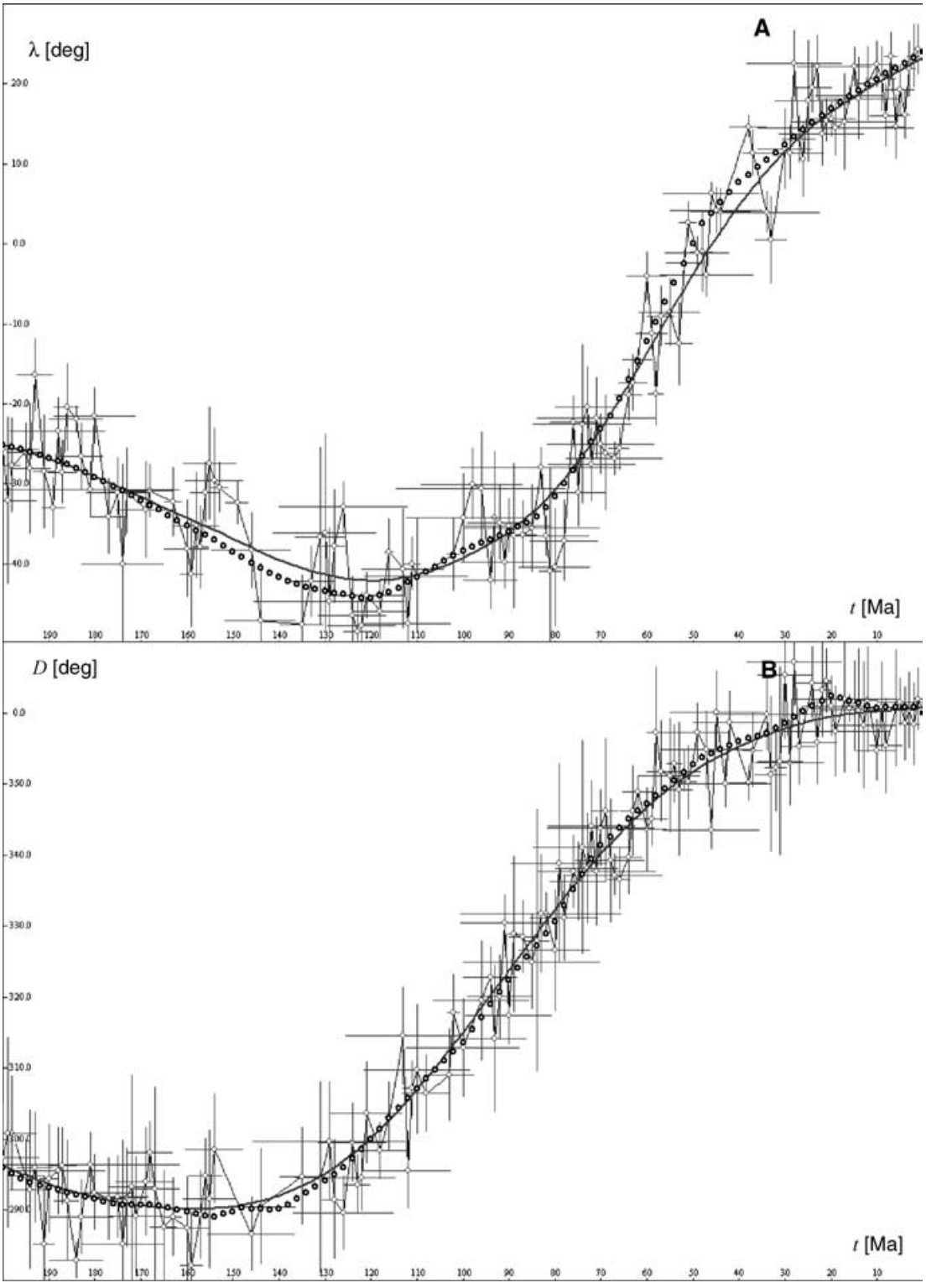

Figure 18. (A) Palaeolatitudes and (B) declinations of a reference point in India at 24°N, 77°E (thin circles with error bars). Solid lines represent spline regression curves with smoothing parameters $\beta_\lambda = \beta_D = 100$. Circles: model-predicted palaeolatitudes (A) and declinations (B).

northwards into south-central Asia, while rotating slightly counterclockwise.

The Indian APW path (Fig. 25) is quite unique and representative of a fast-moving plate. Again, only two segments (tracks) are easily identified: 200–130 Ma and 130 Ma to the present day. However, APW rates show that a relevant change occurred at about 40 Ma.

5.5 Africa

Figs 19(a) and (b) show results for the Central African Craton (reference site near Kisangani, Congo, 0°N, 25°E). Three phases of movement and rotation are clearly distinguishable. During the first phase (200–146 Ma) Africa rotated clockwise (∼22°) about the

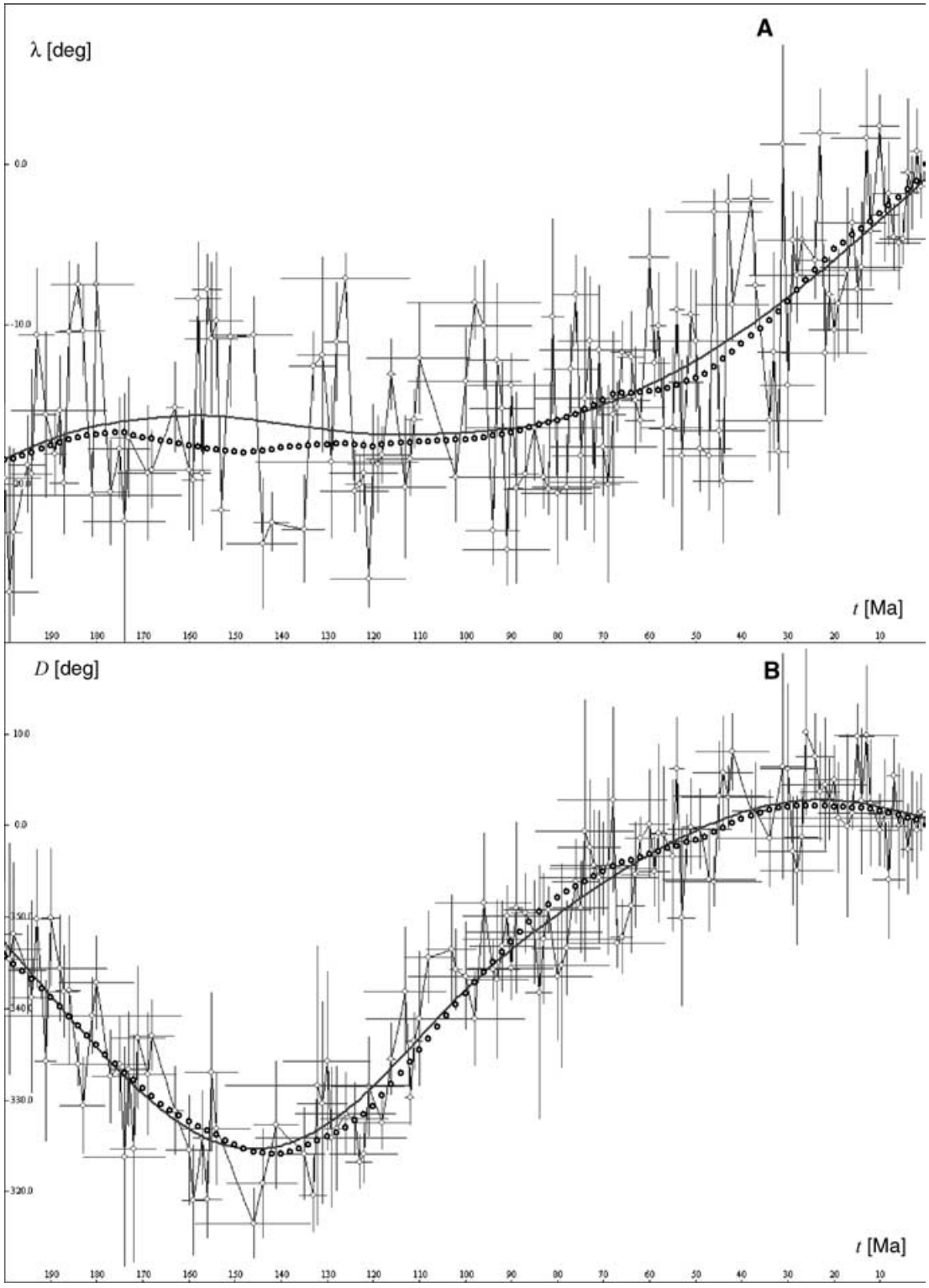

Figure 19. (A) Palaeolatitudes and (B) declinations of a reference point in Central Africa at 0°N, 25°E (thin circles with error bars). Solid lines represent spline regression curves with smoothing parameters $\beta_\lambda = 200$ and $\beta_D = 100$. Circles: model-predicted palaeolatitudes (A) and declinations (B).

reference site. However, the palaeolatitude of this reference point did not change significantly. During the next phase, from 146 to 70 Ma, the palaeomagnetic data suggest that the reference site of Central Africa still retained its palaeolatitude, while the whole continent was rotating strongly counter-clockwise (∼29°). The last phase of movement (70 Ma to the present) is characterized by the northward motion of Central Africa (∼15°) and continuing counter-clockwise rotation, though at a slower rate.

Fig. 26 illustrates the Central African APW path. This APW path is especially interesting because the path appears to double-back on itself at the 146 Ma cusp. The APW path clearly shows all three motion phases.

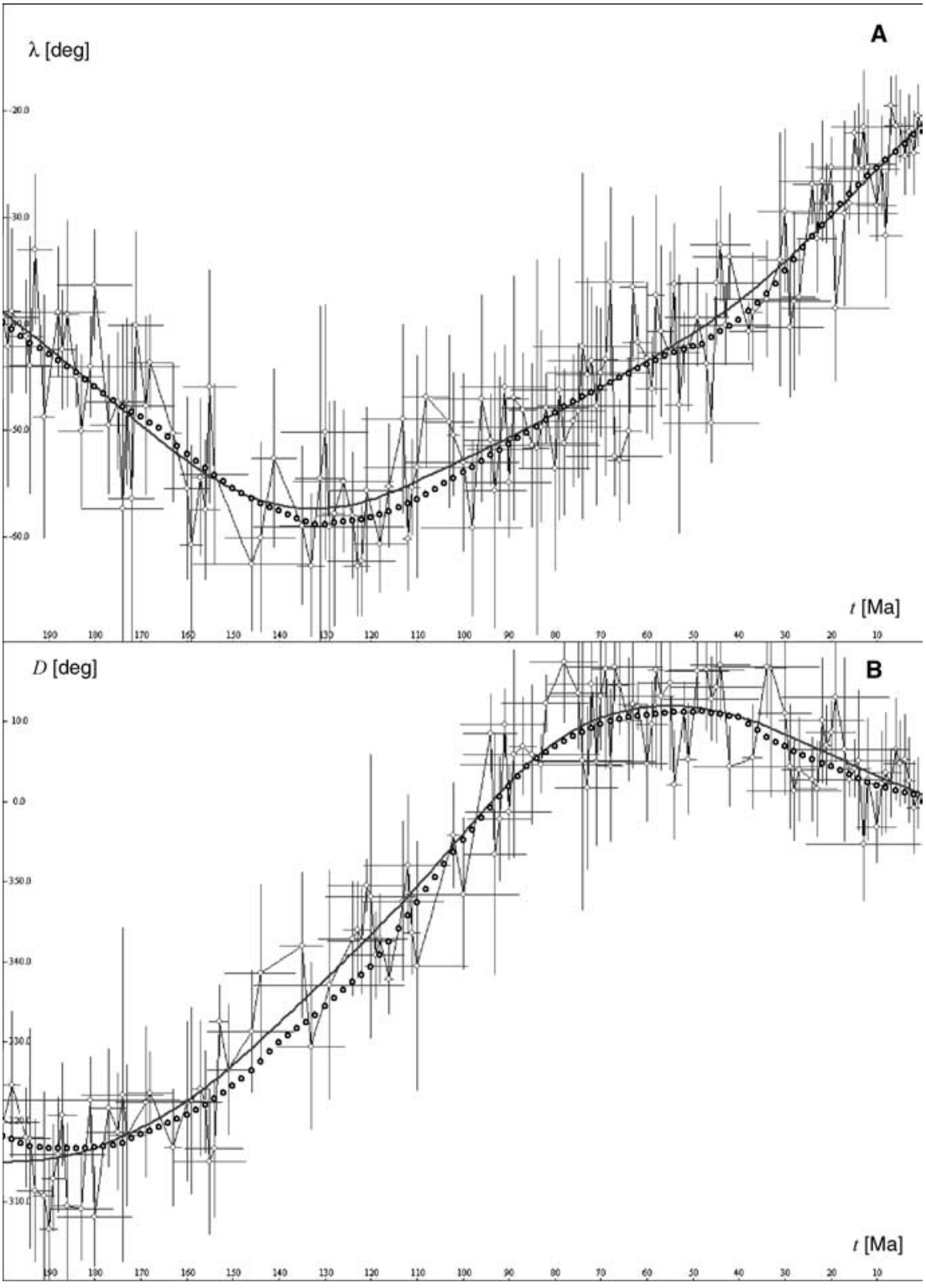

Figure 20. (A) Palaeolatitudes and (B) declinations of a reference point in Australia at 22°S, 134°E (thin circles with error bars). Solid lines represent spline regression curves with smoothing parameters $\beta_\lambda = \beta_D = 100$. Circles: model-predicted palaeolatitudes (A) and declinations (B).

5.6 Australia

Palaeolatitude and declination plots of Central Australia (Alice Springs, 22°S, 134°E) (Figs 20a and b) show southerly movement of the continent (∼18°) between 200 and 134 Ma. During this first phase, Central Australia rotated ∼20° counter-clockwise. The second phase of motion, 135 to 70 Ma, was characterized by northward movement (∼11°) and continuing counter-clockwise rotation. Finally, during the third phase of movement (70 Ma to the present), Australia appears to have accelerated slightly northwards, and reversed its direction of rotation (counter-clockwise to clockwise).

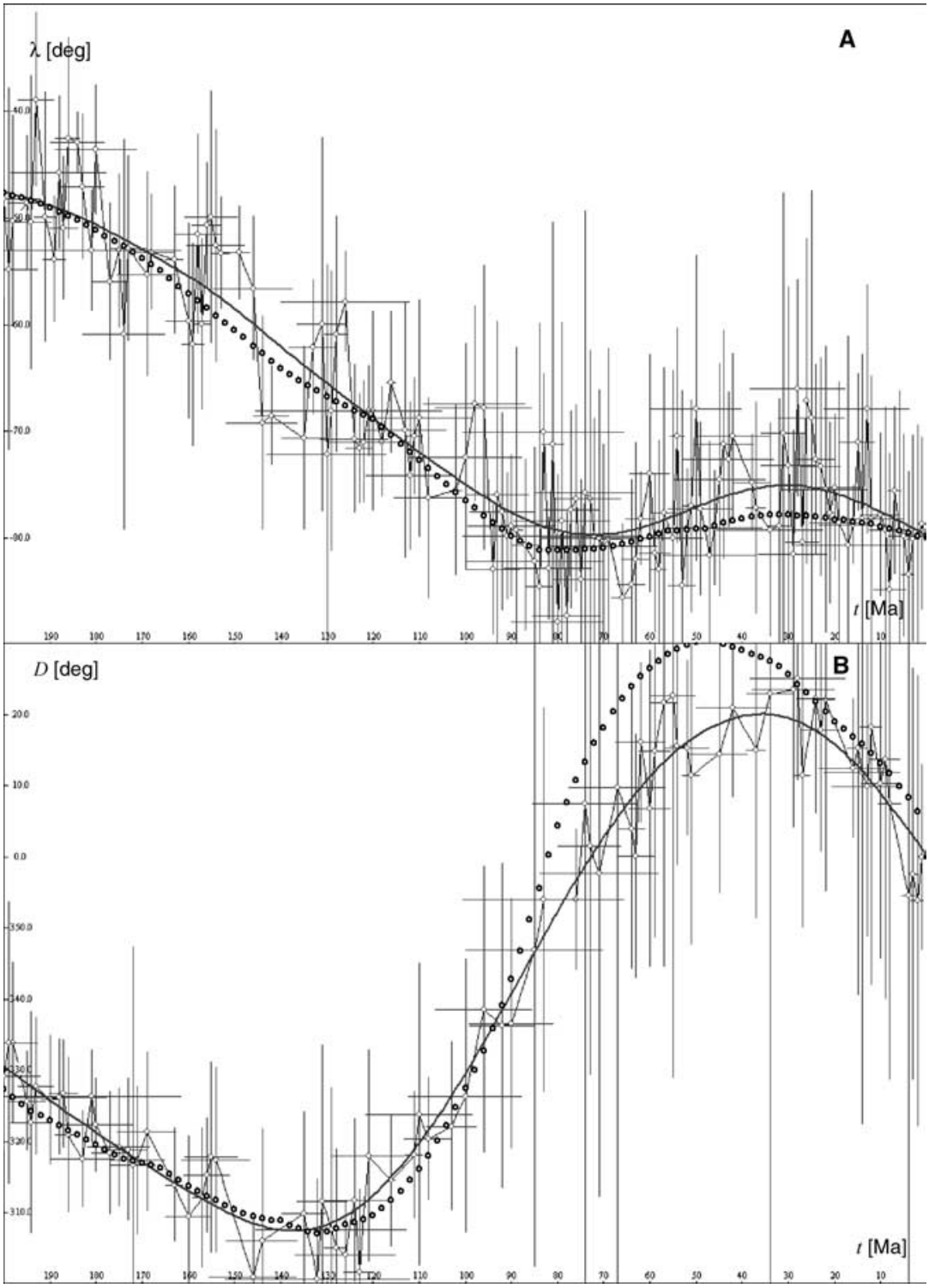

Figure 21. (A) Palaeolatitudes and (B) declinations of a reference point in Antarctica at 80°S, 85°E (thin circles with error bars). Solid lines represent spline regression curves with smoothing parameters $\beta_\lambda = \beta_D = 100$. Circles: model-predicted palaeolatitudes (A) and declinations (B).

The two bends in the APW path for Australia (Fig. 27), at 140–130 Ma and 70–60 Ma, correlate with the timing of similar transitions seen in the palaeolatitude and declination diagrams (Figs 20a and b).

5.7 Antarctica

The last continent we will consider is Antarctica (Figs 21a and b). In this instance the declination and palaeolatitude curves for the reference site (80°S, 85°E) show four distinct phases. During the first phase, 200 to 138 Ma, Antarctica moved ∼1712 km towards the South Pole at a rate 26.8 km Myr^{-1} and rotated slowly clockwise. During the second phase of motion, between 138 and 73 Ma, Antarctica rapidly rotated counter-clockwise (∼55°) and continued its southward movement (1835 km at ∼27.4 km Myr^{-1}). The total southward displacement of Antarctica from the Early Jurassic to the

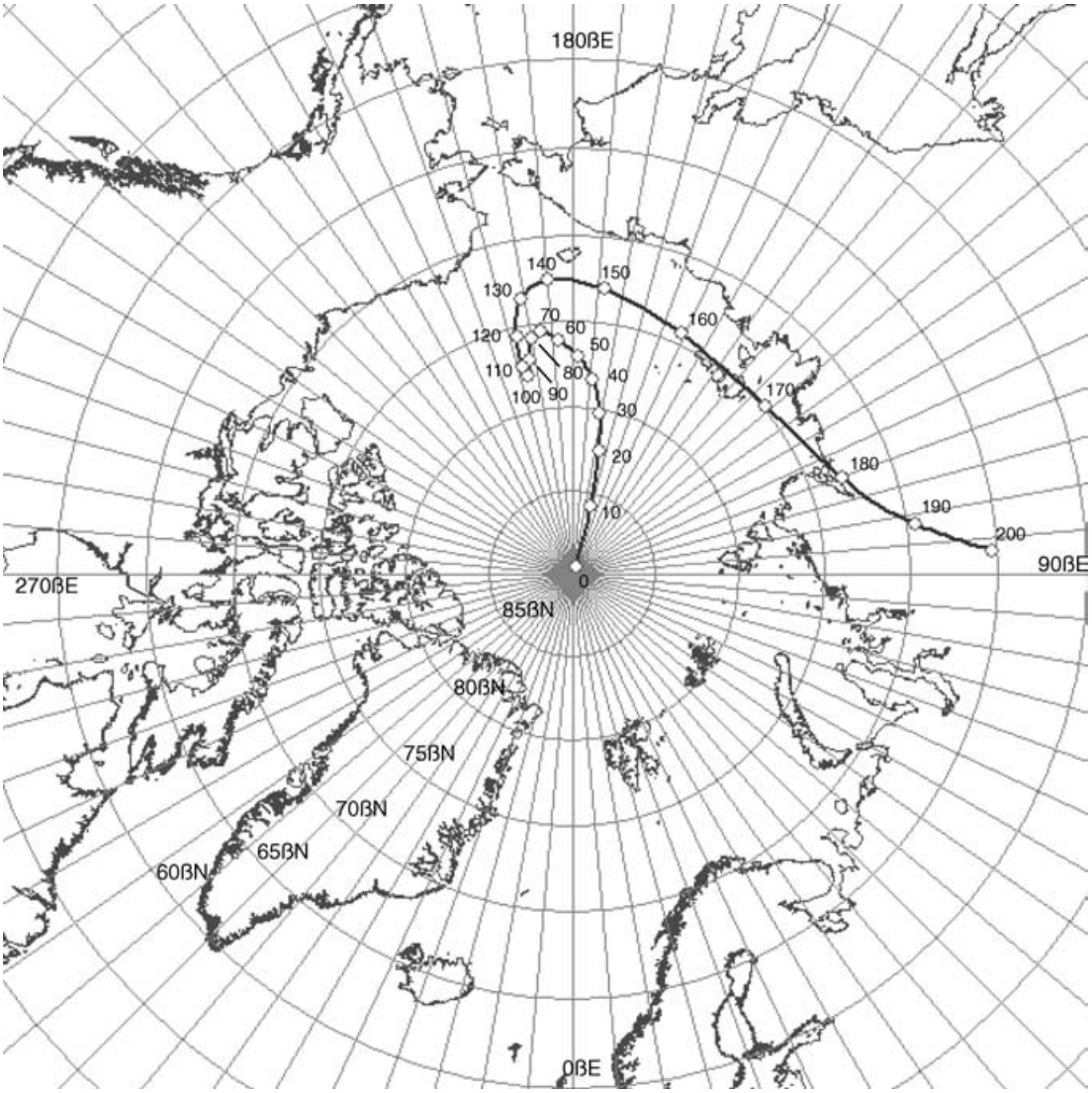

Figure 22. Smoothed apparent polar wander path of North America since the Early Jurassic. Ages are in Ma.

end of the Cretaceous was ∼3547 km. The next phase of motion, from 73 to 34 Ma, was characterized by slow counter-clockwise rotation and increasing palaeolatitudes of the reference point. Finally, from 34 Ma to the present the reference site restarted the southward motion, but the whole continent was subject to fast clockwise rotation about the vertical axis (∼20°).

The Antarctic APW path (Fig. 28) shows the same changes in direction at 140 and 70 Ma. Note that at the end of the Cretaceous the palaeopole position practically coincides with the present day geographical north. Hence, the Cenozoic tract of this APW path can be considered as a narrow loop having a cusp at ∼30 Ma.

5.8 Tectonic phases

Table 12 summarizes the times at which plate motions changed. These transitions were identified by changes in the shape of the palaeolatitude/declination plots and APW paths. We can distinguish only two global events, one at ∼140–120 Ma (Upper Berriasian – Barremian) and another at ∼80–60 Ma (Campanian–Danian). We can also see that local events affected the tectonic regime of North America during the mid-Cretaceous (102 Ma, Upper Albian), South America (48 Ma, Early Lutetian) and Antarctica (34 Ma, Eocene–Oligocene boundary).

In summary, we recognize three major phases of global plate motion since the Early Jurassic. The first phase begins at the J1 cusp (200 Ma) (Molina-Garza *et al.* 1995) and lasts until ∼135 Ma. A second phase runs from ∼135 Ma to ∼70 Ma. The last phase (Phase 3) extends from the latest Cretaceous to the Recent (∼70 Ma to the present day).

6 COMBINING ALL SYNTHETIC APW PATHS IN AFRICAN COORDINATES

In order to define the single, best, palaeomagnetic reference frame, we rotated all of the mean palaeopoles that make up the synthetic APW paths (Figs 22–28) into African coordinates (Fig. 29). This operation was also performed to test the self-consistency of the model and robustness of the procedure explained above. Finally, we calculated a representative best-fit APW path to be used for the assignment of finite reconstruction poles to Central Africa, by vector averaging the seven synthetic palaeopoles associated with

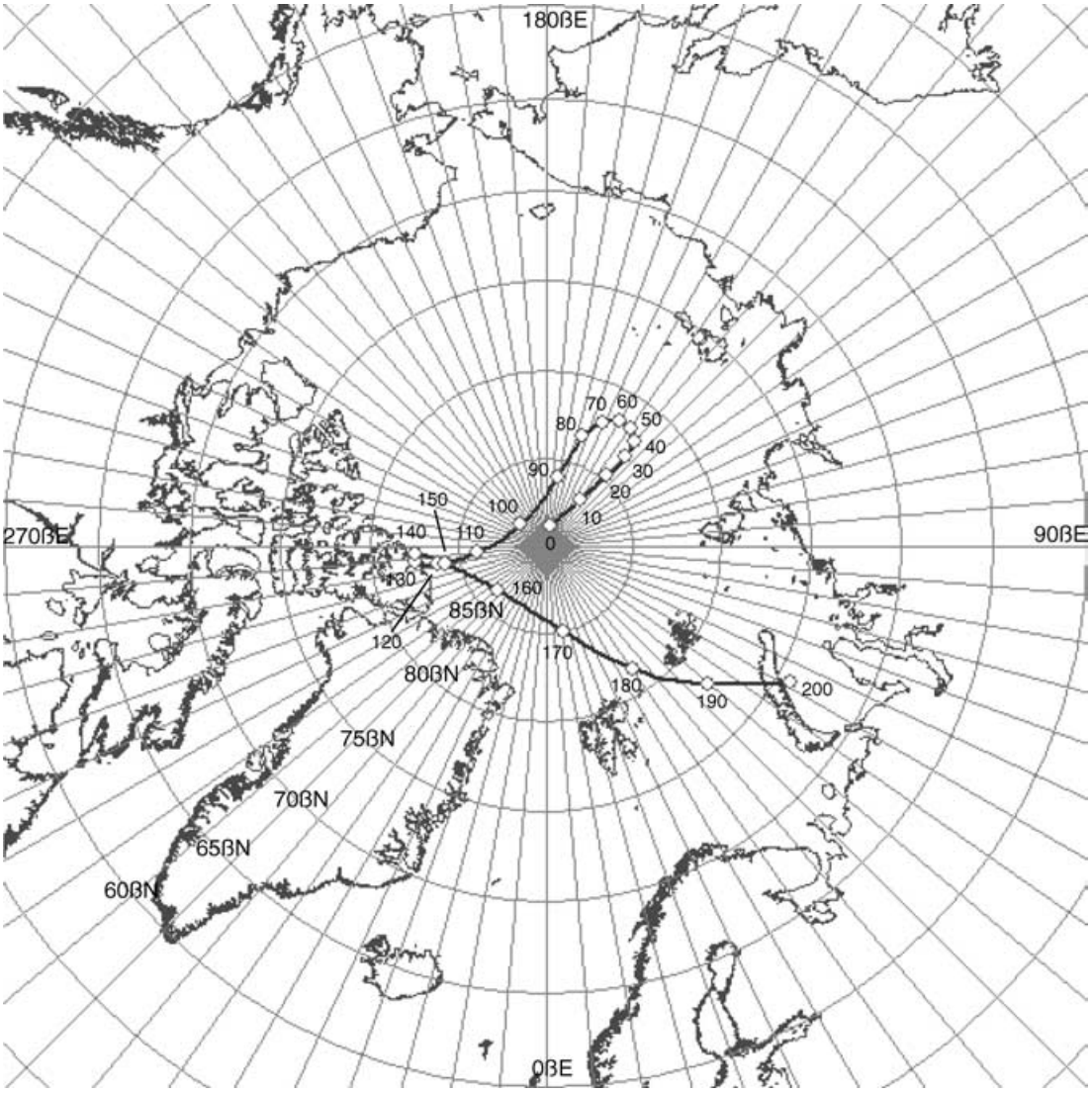

Figure 23. Smoothed apparent polar wander path of South America since the early Jurassic. Ages are in Ma.

each continent. This calculation was carried out for each time t between 200 Ma and 1 Ma at intervals of 1 Myr.

As expected, this global APW path is very similar to the synthetic APW path for Africa (Fig. 26). Table 13 lists the rotated coordinates of all of the mean palaeopoles and the resulting global mean palaeopole (all in African coordinates). The finite rotations that restore the global mean palaeopoles to the spin axis reference frame are given in Table 14. (Tables 13 and 14 are available in the online version of this article only.) The resulting rotation model describes the movement of Africa from 200 Ma to the present.

A comparison between the global APW path (African coordinates) and the APW path proposed by Besse & Courtillot (2002) for Africa is shown in Fig. 30. We note that the APW path proposed by these authors is affected by the well-known far-side effect (e.g. Merrill & McElhinny 1983) on Miocene to Recent palaeopoles, whereas the curve obtained in this paper does not. This feature depends on the boundary conditions assumed in the post-filtering procedure (eq. 6). In Figs 15–21 model-predicted palaeolatitudes and declinations are compared with curves resulting from regression analysis. The agreement is good, with the exception of Late Cretaceous to Eocene declinations of Antarctica. This discrepancy seems to be related to the removal of too many high-declination palaeopole components, which was necessary to satisfy the boundary condition (eq. 6). Hence, we believe that the model-predicted trend, and not the regression curve, furnishes a better representation of the tectonic history of this plate.

7 PLATE TECTONIC RECONSTRUCTIONS FOR THE THREE GLOBAL PLATE MOTION REGIMES

We have shown that two important events of global plate reorganization occurred at 135 and 70 Ma. These events mark the boundaries of three distinct phases of global plate motions since the Early Jurassic. The four plate tectonic reconstructions in Figs 31–34 illustrate the main features of the tectonic regime during these phases. The reconstructions show the global plate velocity field in the palaeomagnetic frame of reference for each time period. The first phase, between 200 and 135 Ma, was characterized by a generalized clockwise rotation of the continental lithosphere (Fig. 31), though the three major fragments of Pangaea (Laurasia, central and southern Gondwana) were moving at different angular velocities. During the

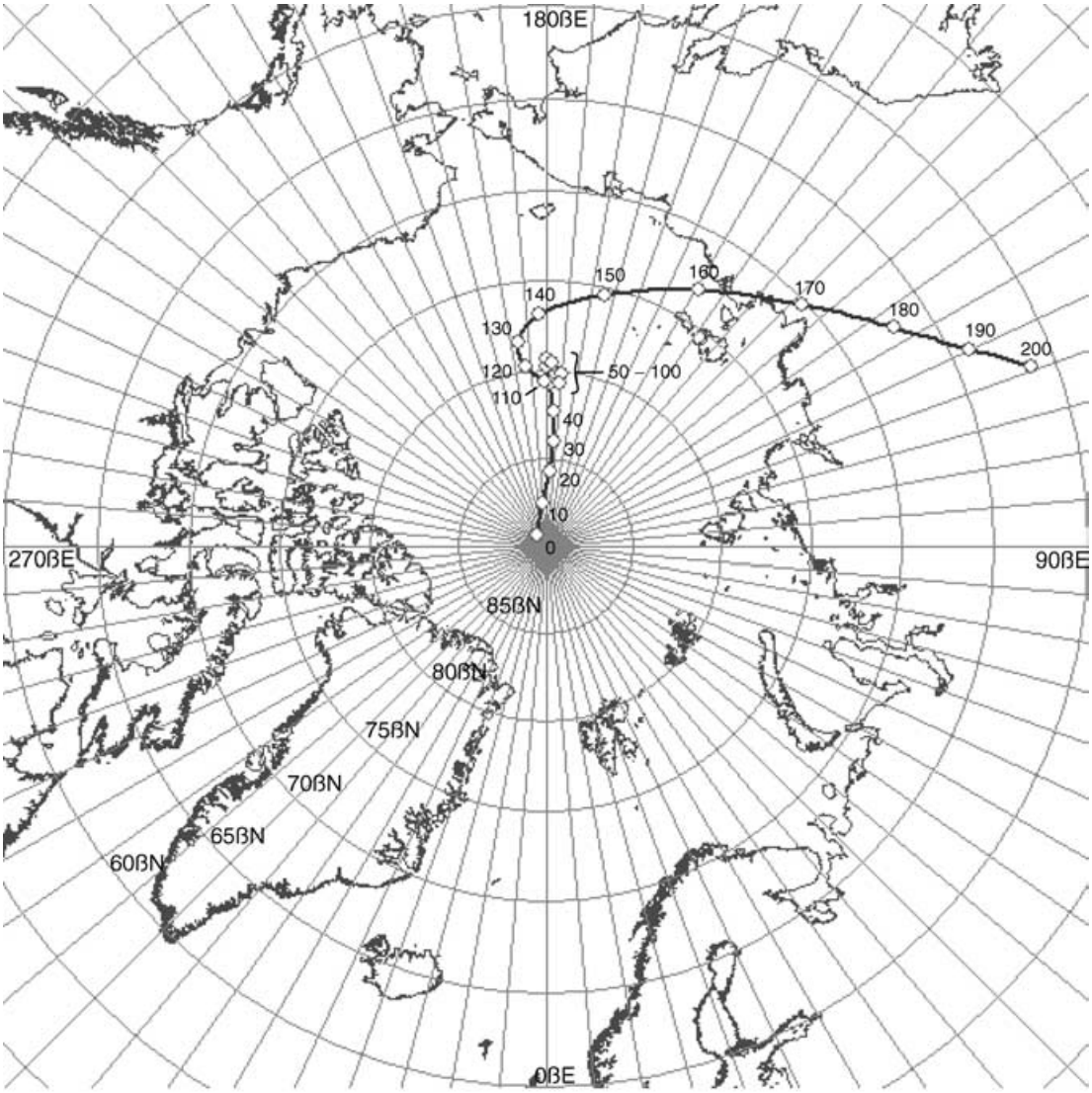

Figure 24. Smoothed apparent polar wander path of Eurasia since the Early Jurassic. Ages are in Ma.

second phase, between 135 and 70 Ma, the global velocity field was initially inverted. In fact, between 135 Ma and anomaly M0 (120.4 Ma, Aptian) we observe a general pattern of counter-clockwise rotation (Fig. 32). However, Fig. 33 shows that at the top of the Cretaceous long normal-polarity chron (C34n) a complex plate velocity field took place, associated with the final phase of Pangaea fragmentation. During the upper part of Phase 2 the only continents that were moving in concert were North America and Eurasia. Both continents rotated clockwise. Finally, the most recent phase, between 70 Ma and the present, appears to be dominated by counter-clockwise rotations, with the exception of the Pacific Plate (Fig. 34).

8 DISCUSSION: HOT SPOT OR PALAEOMAGNETIC REFERENCE FRAME—WHICH IS BETTER?

A plate tectonic reconstruction for any time t is calculated using a hierarchical structure that describes the relative motion between pairs of plates using finite Euler rotations. This hierarchical structure is also known as a 'plate circuit'. In this tree-like structure, a reference continent occupies the topmost node. The motion of the reference continent is defined with respect to an external reference frame. The identification of a physically meaningful external reference frame is still one of the greatest challenges in plate tectonic modelling. During the past three decades, three different methods have been used, each suggesting a different external frame of reference.

The standard palaeomagnetic reference frame is uniquely based upon the geocentric axial (but not necessarily dipolar) hypothesis and the determination of an APW path for the reference plate. Palaeopositions of the reference continent are calculated assuming no relation between consecutive points on the APW paths. In fact, this method requires the selection of an arbitrary point (λ_0, φ_0) on the reference plate at time $t = 0$. Then, the finite rotations corresponding to each palaeopole position are independently obtained by applying the transformation:

$$\mathbf{R}(t) = \mathbf{R}(0, \varphi_0 + 90, \lambda_0 - \lambda(t))\mathbf{R}(\lambda_0, \varphi_0, D(t)). \quad (10)$$

In this equation, $\mathbf{R}(t)$ represents the finite rotation (in matrix form) that must be applied to points on the reference continent to restore their orientations and palaeolatitudes at time t, $\mathbf{R}(\lambda, \varphi, \omega)$ is a rotation about the generic Euler pole (λ, φ) by an angle ω (e.g. Cox

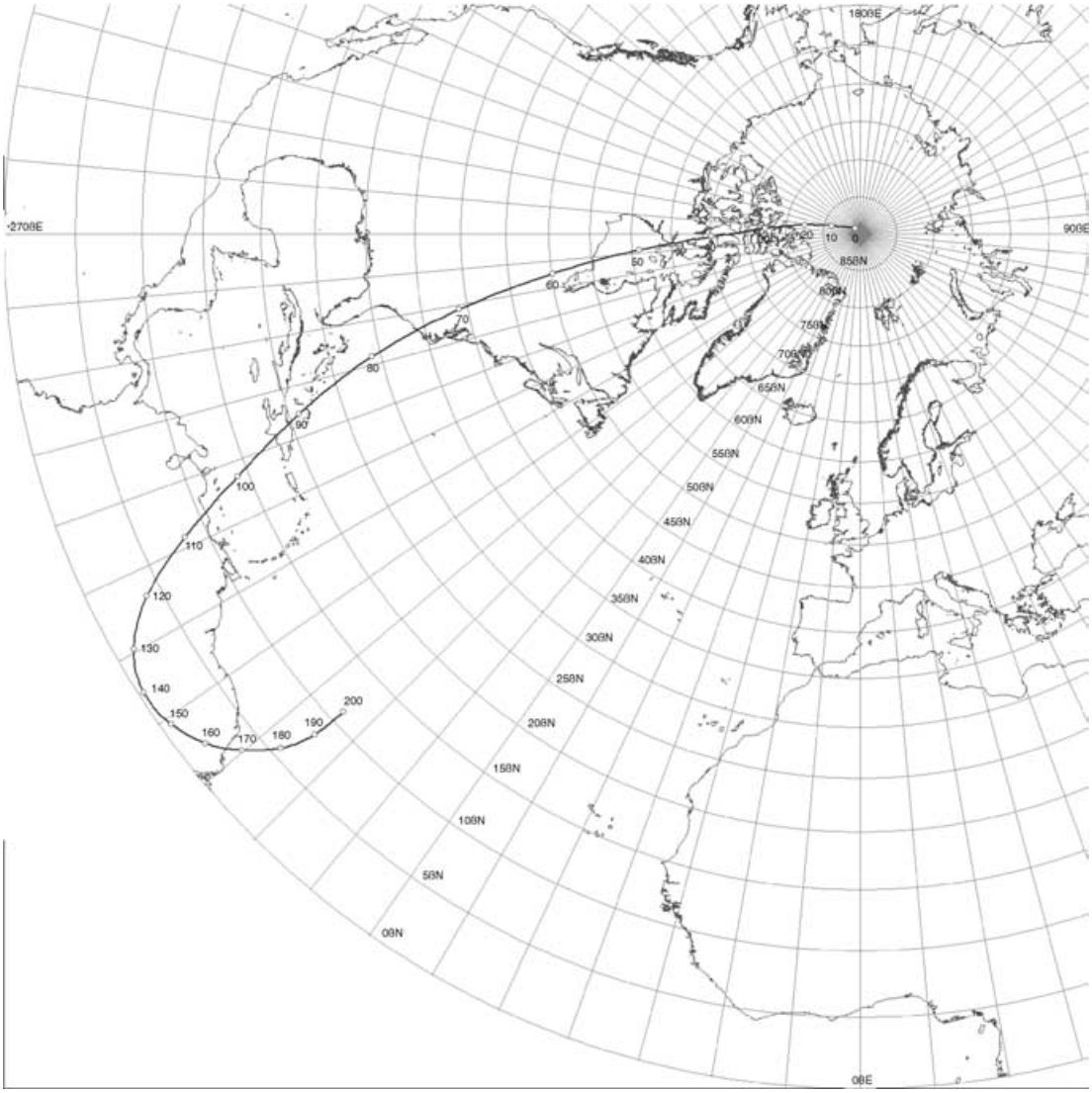

Figure 25. Smoothed apparent polar wander path of India since the Early Jurassic. Ages are in Ma.

& Hart 1986) and $D(t)$ and $\lambda(t)$ are respectively the declination of the reference point and its palaeolatitude at time t, as determined by the palaeopole position (e.g. Van der Voo 1993). An application of this method can be found in Besse & Courtillot (1988). It should be noted that this approach leaves invariant the longitude of the reference point for each reconstruction time.

In an alternative, but substantially equivalent, reconstruction technique each finite pole of rotation is simply defined as the rotation that is necessary to move a palaeopole from the APW path to the geographical North Pole along a meridian of longitude. In this instance, all the resulting total reconstruction poles lie along the Equator, but individual palaeopoles are still seen as independent of each other and palaeolongitudes remain undetermined. A classic example of the use of such a reference frame is given by Ziegler *et al.* (1983).

Most authors recognize that palaeomagnetic data can only constrain palaeolatitudes and azimuthal orientations of continental blocks, and that they do not provide any information about longitude. This is certainly true if we consider isolated palaeopoles, as well as if we neglect any information about the geometry of an APW path. In the framework of the palaeomagnetic Euler pole (PEP) analysis (Gordon *et al.* 1984), some geometrical properties are assumed for the APW paths, and consecutive palaeopoles are considered to be 'linked'. PEP analysis assumes that any APW path is a spherical curve composed of tracks corresponding to stages of constant motion about fixed Euler poles (the PEPs). The cusps in the PEP path correspond to times of rapid change in the plate motion. In other words, it is assumed that the geometry of any APW path can be described as a sequence of small circles about changing Euler poles. If this description is correct, then this method allows for the resolution of all three components of motion. This conclusion, however, remains controversial (e.g. Van der Voo 1993).

The third widely used approach to describe the motion of the plates with respect to an external frame of reference is based upon the fixed hot spot hypothesis (Morgan 1971) and on the analysis of hot spot tracks, which are supposed to record the motion of tectonic plates over stationary 'hot spots' (Duncan 1981; Morgan 1983; Gordon 1983; Duncan 1984; O'Connor & Duncan 1990; Müller *et al.* 1993). This approach applies only to Cretaceous and Cenozoic reconstructions, because of the scarcity of hot spot data for older times. Moreover, though a consistent set of rotation parameters which describes the motions of the plates bordering the Atlantic and Indian oceans can be found (Müller *et al.* 1993), this technique cannot be

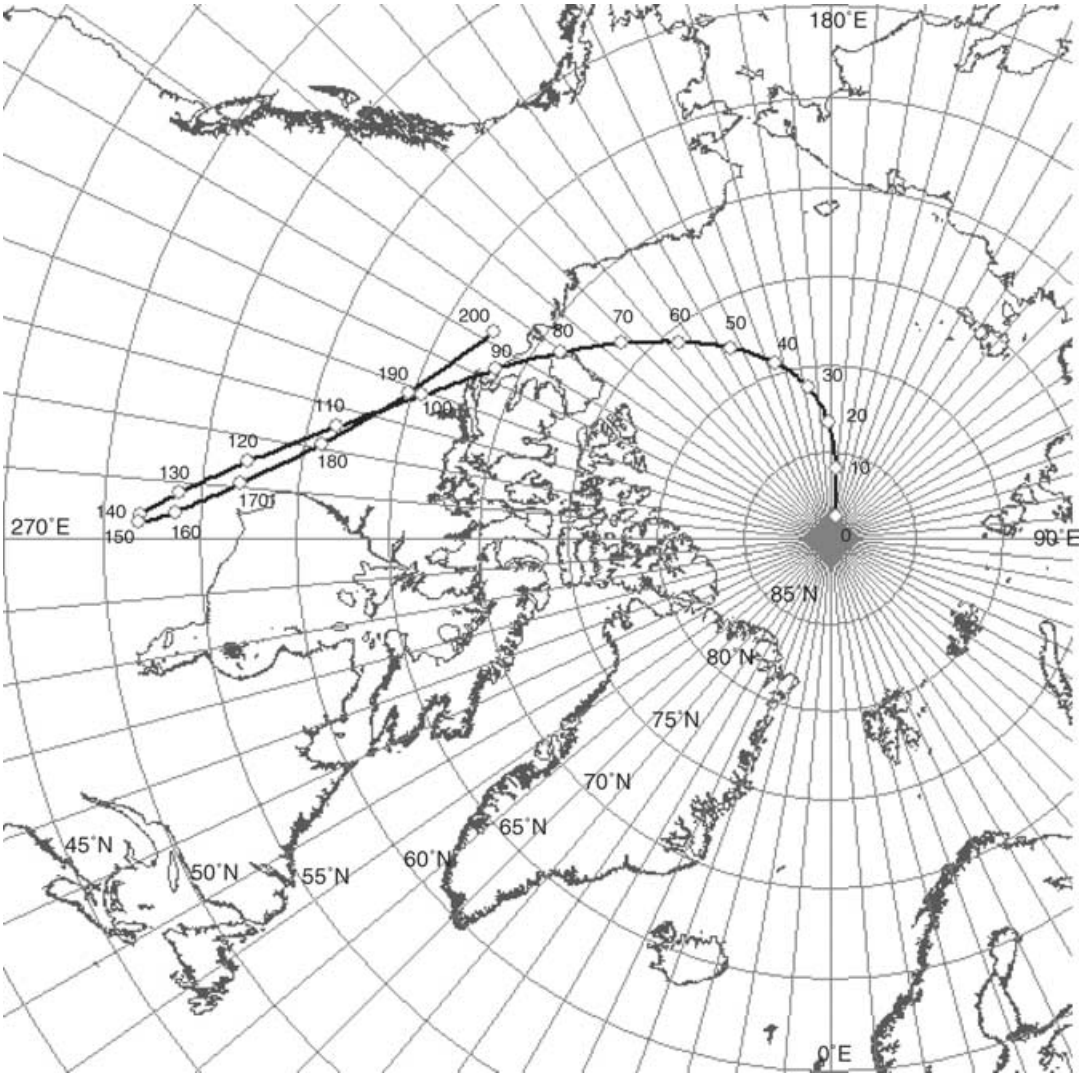

Figure 26. Smoothed apparent polar wander path of Central Africa since the Early Jurassic. Ages are in Ma.

extended to include Pacific hot spot tracks, because these hot spots appear to have moved with respect to Atlantic and Indian Ocean hot spots (Molnar & Stock 1987). This implies that the hot spot reference frame, while locally useful, does not constitute a coherent, global reference frame. The hot spot reference frame, nevertheless, has been used to test for episodes of true polar wander (TPW), which would be recorded as absolute displacements of the spin axis in the hot spot frame of reference.

The choice of a palaeomagnetic reference frame, rather than a hot spot reference frame, is justified by the following considerations. During the last two decades several attempts have been made to represent global plate tectonic reconstructions in the hot spot reference frame (e.g. Duncan 1981; Morgan 1983; Schult & Gordon 1984; Duncan 1984; Gordon & Jurdy 1986; O'Connor & Duncan 1990; Müller *et al.* 1993). However, recent studies have demonstrated that:

(1) Hot spots are not generally fixed with respect to each other (Molnar & Stock 1987; DiVenere & Kent 1999).

(2) Hot spots are moving with respect to the spin axis (e.g. Gordon & Cape 1981; Andrews 1985; Tarduno & Cottrell 1997).

(3) Mantle plumes might be subject to distortion by advection in a large-scale mantle flow, resulting in the migration of the hot spots with respect to the deep mantle (Steinberger & O'Connell 1998; Christensen 1998).

Nevertheless, selected groups of hot spots reveal a coherent behaviour for long time periods, as has been demonstrated in the case of the Atlantic and Indian Ocean hot spot tracks (Müller *et al.* 1993).

We realize that the palaeomagnetic reference frame described here is not an absolute reference frame. Nevertheless, we believe that it comes close to satisfying the requirements of such a reference frame. We hope that further research comparing the global palaeomagnetic reference frame proposed here with the hot spot reference frame will shed light on the nature of hot spots, will help to define the relationship between groups of hot spots, and will ultimately result in the reconciliation of the palaeomagnetic and hot spot frames of reference.

9 CONCLUSIONS

In this paper we have presented a new technique to analyse palaeomagnetic data and to produce smoothed, synthetic APW paths. The goal of this paper has been to define a palaeomagnetic reference frame that can be used as a framework to describe global plate motions. We believe that the smoothed curves of palaeolatitude and

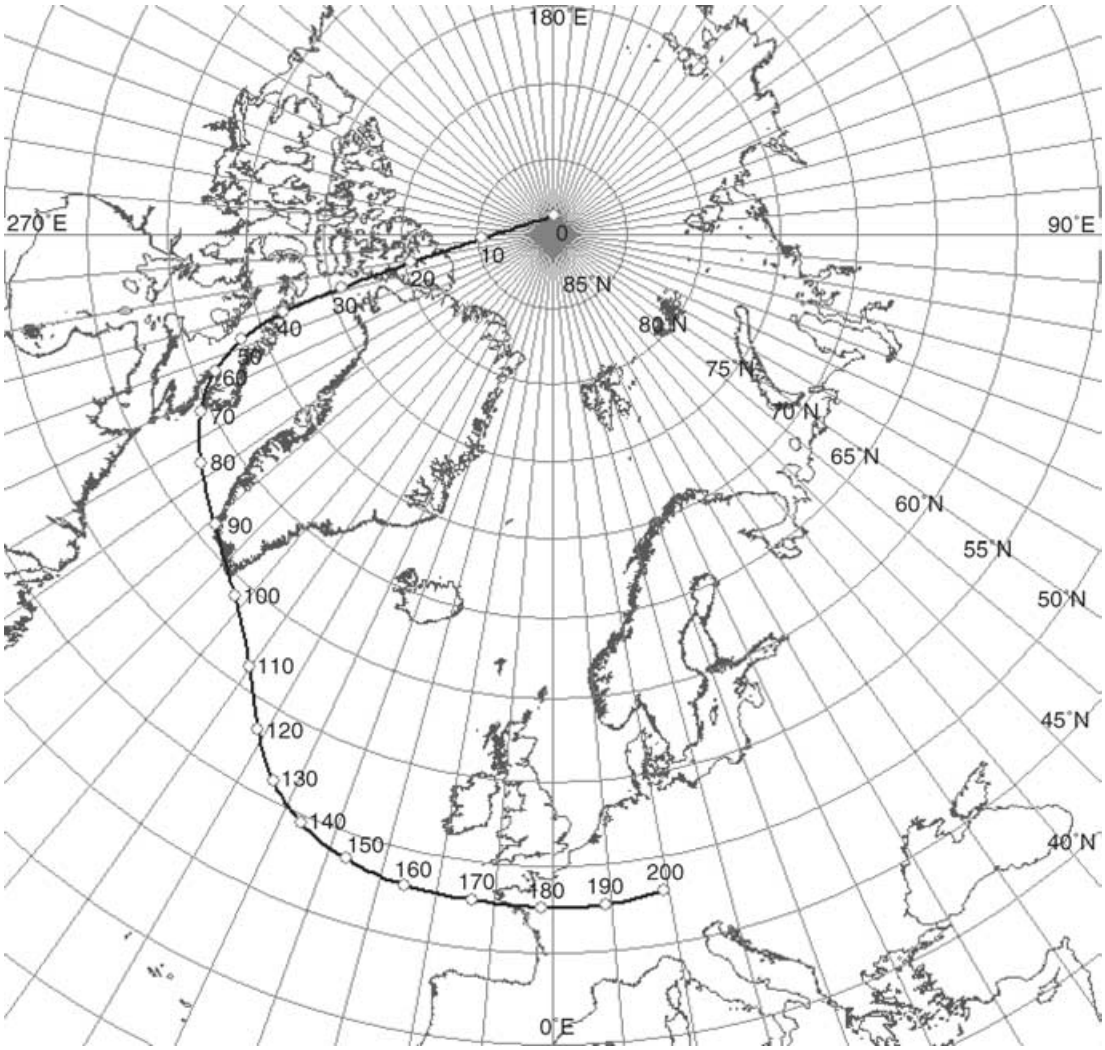

Figure 27. Smoothed apparent polar wander path of Australia since the Early Jurassic. Ages are in Ma.

declination, as well as the synthetic APW paths derived from these curves, provide an accurate description of global plate motions since the Early Jurassic. The regression curves and APW paths fit the available palaeomagnetic data and are consistent with the gradually changing pattern of plate motion during the last 200 Myr.

ACKNOWLEDGMENTS

The authors would like to thank R. Van der Voo and R. Butler for their palaeomagnetic insights through the years. We would also like to thank B. Steinberger for his constructive comments and criticisms that improved a preliminary version of this paper. Finally, we thank R. Van der Voo and D. Kent for their very careful and useful reviews. This work was funded in part by sponsors of the PALEOMAP Project, University of Texas at Arlington.

REFERENCES

Acton, G.D., Petronotis, K.E., Cape, C.D., Ilg, S.R., Gordon, R.G. & Bryan, P.C., 1996. A test of the geocentric axial dipole hypothesis from an analysis of the skewness of the central marine magnetic anomaly, *Earth planet. Sci. Lett.,* **144,** 337–346.

Andrews, J.A., 1985. True polar wander: an analysis of Cenozoic and Mesozoic paleomagnetic poles, *J. geophys. Res.,* **90**(B9), 7737–7750.

Bazard, D.R. & Butler, R.F., 1994. Paleomagnetism of the Brushy Basin Member of the Morrison Formation: implications for Jurassic apparent polar wander, *J. geophys. Res.,* **99**(B4), 6695–6710.

Besse, J. & Courtillot, V., 1988. Paleogeographic maps of the continents bordering the Indian Ocean since the early Jurassic, *J. geophys. Res.,* **93**(B10), 11 791–11 808.

Besse, J. & Courtillot, V., 1991. Revised and synthetic apparent polar wander paths of the African, Eurasian, North American and Indian plates, and true polar wander since 200 Ma, *J. geophys. Res.,* **96**(B3), 4029-4050.

Besse, J. & Courtillot, V., 2002. Apparent and true polar wander and the geometry of the geomagnetic field over the last 200 Myr, *J. geophys. Res.,* **107**(B11), 2300, doi:10.1029/2000JB000050.

Blakely, R.J., 1995. *Potential Theory in Gravity and Magnetic Applications*, Cambridge University Press, Cambridge.

Bocharova, N.Y. & Scotese, C.R., 1993. *Revised Global Apparent Polar Wander Paths and Global Mean Poles*, Paleomap Project progress report no 56, Department of Geology, University of Texas at Arlington, TX.

Brewer, T.S., Rex, D., Guise, P.G. & Hawkesworth, C.J., 1996. Geochronology of Mesozoic tholeiitic magmatism in Antarctica: implications for the development of the failed Weddel Sea rift system, in *Weddel Sea Tectonics and Gondwana Break-up*, Geological Society Special Publication 108, pp. 45–61, eds Storey, B.C., King, E.C. & Livermore, R.A., The Geological Society, London.

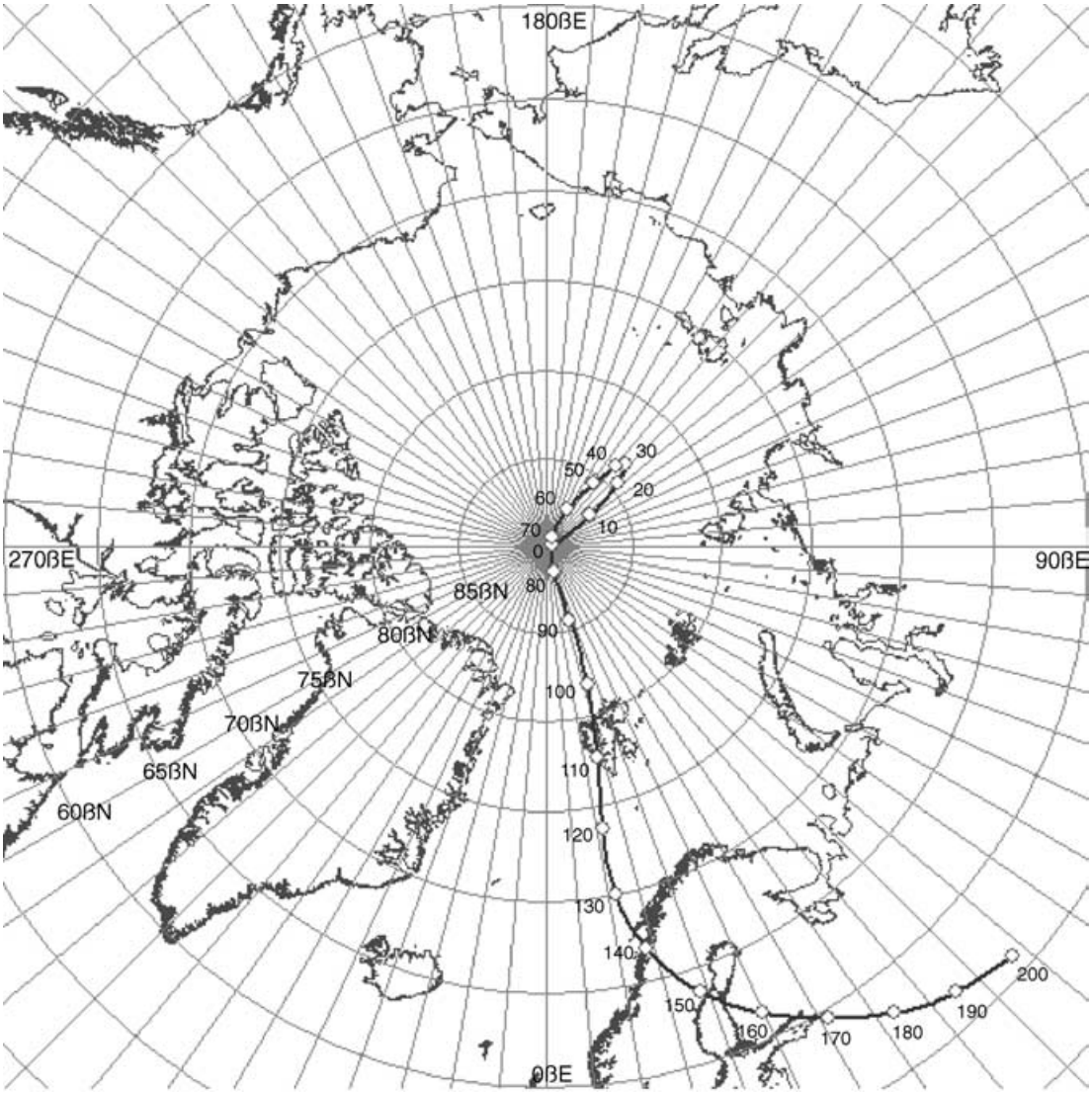

Figure 28. Smoothed apparent polar wander path of East Antarctica since the Early Jurassic. Ages are in Ma.

Table 12. Phase boundaries identified on palaeolatitude/declination plots and APW paths.

Plate	Name	J1	K1	uK1	Ku	E2
101	North America	200	138	102	73	
201	South America	200	137		74	48
301	Eurasia	200	135		72	
501	India	200	130			
701	Central Africa	200	146		70	
801	Australia	200	134		70	
802	Antarctica	200	138		73	34

J1, Early Jurassic; K1, Early Cretaceous; uK1, Late Early Cretaceous; Ku, Upper Cretaceous; E2, Eocene. Ages are in Ma.

Butler, R.F., 1992. *Paleomagnetism: Magnetic Domains to Geologic Terranes*, Blackwell Scientific, Oxford.

Christensen, U., 1998. Fixed hotspots gone with the wind. *Nature,* **391,** 739–740.

Coffin, M.F. & Eldholm, O., 1994. Large igneous provinces: crustal structure, dimensions, and external consequences, *Rev. Geophys.,* **32,** 1–36.

Cox, A. & Hart, R.B., 1986. *Plate Tectonics: How it Works*, Blackwell Scientific, Palo Alto, CA.

DeMets, C., Gordon, R.G., Argus, D.F. & Stein, S., 1994. Effect of recent revisions to the geomagnetic reversal time scale on estimate of current plate motions, *Geophys. Res. Lett.,* **21**(20), 2191–2194.

DiVenere, V. & Kent, D.V., 1999. Are the Pacific and Indo-Atlantic hotspots fixed? Testing the plate circuit through Antarctica, *Earth planet. Sci. Lett.,* **170,** 105–117.

Duncan, R.A., 1981. Hot-spots in the southern oceans—an absolute frame of reference for the motion of the Gondwana continents, *Tectonophysics,* **74,** 29–42.

Duncan, R.A., 1984. Age progressive volcanism in the New England seamounts and the opening of the central Atlantic Ocean, *J. geophys. Res.,* **89**(B12), 9980–9990.

Ebinger, C.J. & Sleep, N.H., 1998. Cenozoic magmatism throughout east Africa resulting from impact of a single plume, *Nature,* **395,** 788–791.

Ekstrand, E.J. & Butler, R.F., 1989. Paleomagnetism of the Moenave Formation: implications for the Mesozoic North American apparent polar wander path, *Geology,* **17,** 245–248.

Eubank, R.L., 1988. *Spline Smoothing and Nonparametric Regression*, Marcel Dekker, New York.

Genik, G.J., 1992. Regional framework, structural and petroleum aspects of rift basins in Niger, Chad and the Central African Republic (C.A.R.), *Tectonophysics,* **213,** 169–185.

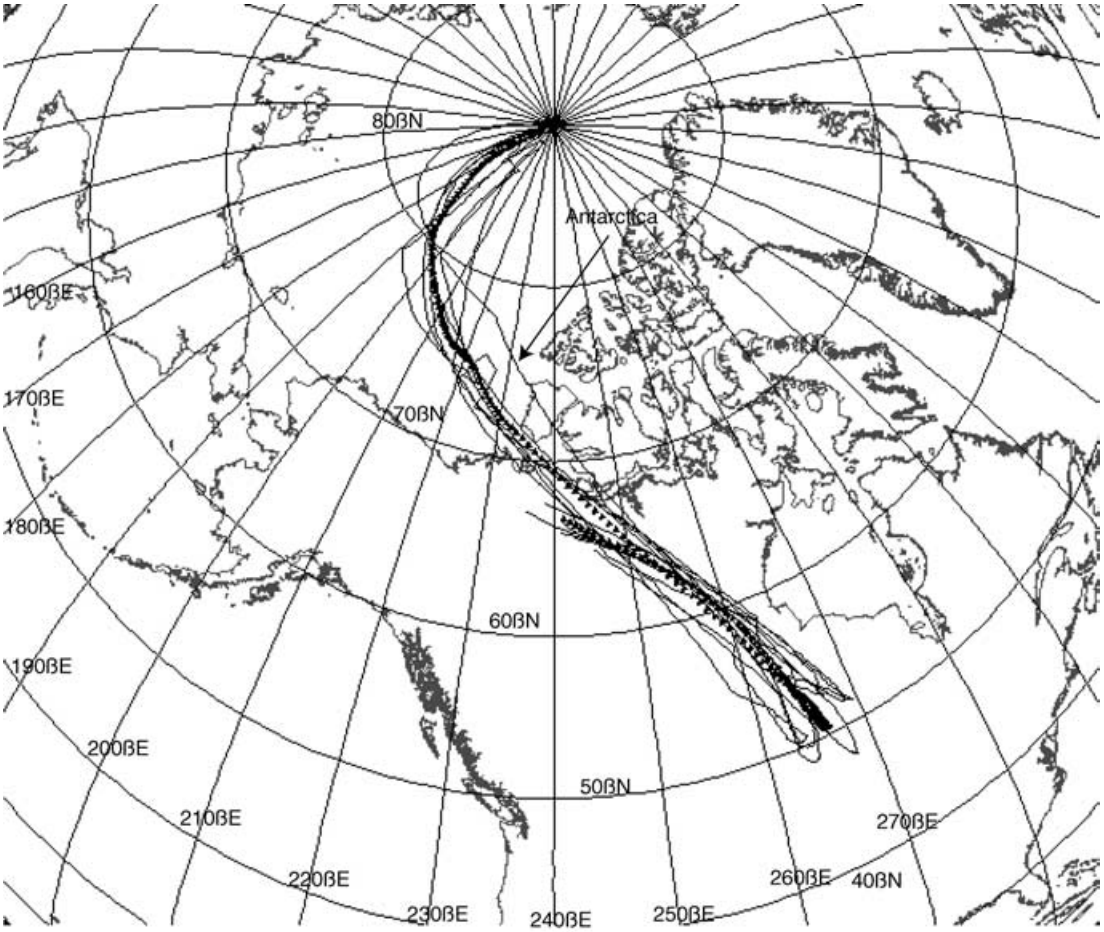

Figure 29. Central African APW path (triangles) and APW paths of North America, South America, Eurasia, India, Australia and Antarctica rotated in Central African coordinates (lines). The representative best-fit African APW path, obtained by Fisherian average of synthetic palaeopoles having the same age, is shown as a sequence of triangles at intervals of 1 Myr. Note the angular separation between the Antarctic APW path and the best-fit curve.

Gordon, R.G., 1983. Late Cretaceous apparent polar wander of the Pacific plate: evidence for a rapid shift of the Pacific hotspots with respect to the spin axis, *Geophys. Res. Lett.,* **10**(8), 709–712.

Gordon, R.G. & Cape, C.D., 1981. Cenozoic latitudinal shift of the Hawaiian hot spot and its implications for true polar wander, *Earth planet. Sci. Lett.,* **55,** 37–47.

Gordon, R.G. & Jurdy, D.M., 1986. Cenozoic global plate motions, *J. geophys. Res.,* **91**(B12), 12 389–12 406.

Gordon, R.G., Cox, A. & O'Hare, S., 1984. Paleomagnetic Euler poles and the apparent polar wander and absolute motion of North America since the Carboniferous, *Tectonics,* **3**(5), 499–537.

Gradstein, F.M. *et al.*, 2004. *Geologic Time Scale 2004*, Cambridge University Press, Cambridge.

Guiraud, R. & Maurin, J.C., 1992. Early Cretaceous rifts of western and central Africa, *Tectonophysics,* **213,** 153–168.

Harrison, C.G.A. & Lindh, T., 1982. A polar wandering curve for North America during the Mesozoic and Cenozoic, *J. geophys. Res.,* **87**(B3), 1903–1920.

Jupp, P.E. & Kent, J.T., 1987. Fitting smooth paths to spherical data, *Appl. Statist.,* **36**(1), 34–46.

Klitgord, K.D. & Schouten, H., 1986. Plate kinematics of the central Atlantic, in *The Geology of North America, Vol. M, The Western North Atlantic Region*, pp. 351–378, eds Vogt, P.R. & Tucholke, B.E., Geological Society of America, Boulder, CO.

Larson, R.L., Pitman, W.C., III, Golovchenko, X., Cande, S.C., Dewey, J.F., Haxby, W.F. & Labrecque, J.L., 1985. *The Bedrock Geology of the World*, Freeman, New York.

Le Pichon, X. & Gaulier, J.M., 1988. The rotation of Arabia and the Levant fault system, *Tectonophysics,* **153,** 271–274.

Livermore, R.A., Vine, F.J. & Smith, A.G., 1983. Plate motions and the geomagnetic field—I. Quaternary and late Tertiary, *Geophys. J. R. astr. Soc,* **73,** 153–171.

Livermore, R.A., Vine, F.J. & Smith, A.G., 1984. Plate motions and the geomagnetic field—II. Jurassic to Tertiary, *Geophys. J. R. astr. Soc,* **79,** 939–961.

Lock, J. & McElhinny, M.W., 1991. Global palaeomagnetic data base: design, installation and use with Oracle. *Surv. Geophys.,* **12,** 317.

Martin, A.K., Hartnady, C.J.H. & Goodlad, S.W., 1981. A revised fit of South America and South Central Africa, *Earth planet. Sci. Lett.,* **54,** 293–305.

McElhinny, M.W. & Lock, J., 1990. Global palaeomagnetic data base project, *Phys. Earth planet. Int.,* **63,** 1–6, 1990.

McElhinny, M.W., McFadden, P.L. & Merrill, R.T., 1996. The time-averaged paleomagnetic field 0–5 Ma, *J. geophys. Res.,* **101**(B11), 25 007–25 027.

Merrill, R.T. & McElhinny, M.W., 1983. *The Earth's Magnetic Field: its History, Origin and Planetary Perspective*, Academic Press, San Diego, CA.

Molina-Garza, R.S., Geissman, J.W. & Van der Voo, R., 1995. Paleomagnetism of the Dockum Group (Upper Triassic), northwest Texas: further evidence for the J-1 cusp in the North America apparent polar wander path and implications for rate of Triassic apparent polar wander and Colorado plateau rotation, *Tectonics,* **14**(4), 979–993.

Molnar, P. & Stock, J., 1987. Relative motions of hotspots in the Pacific, Atlantic and Indian oceans since Late Cretaceous time, *Nature,* **327,** 587–591.

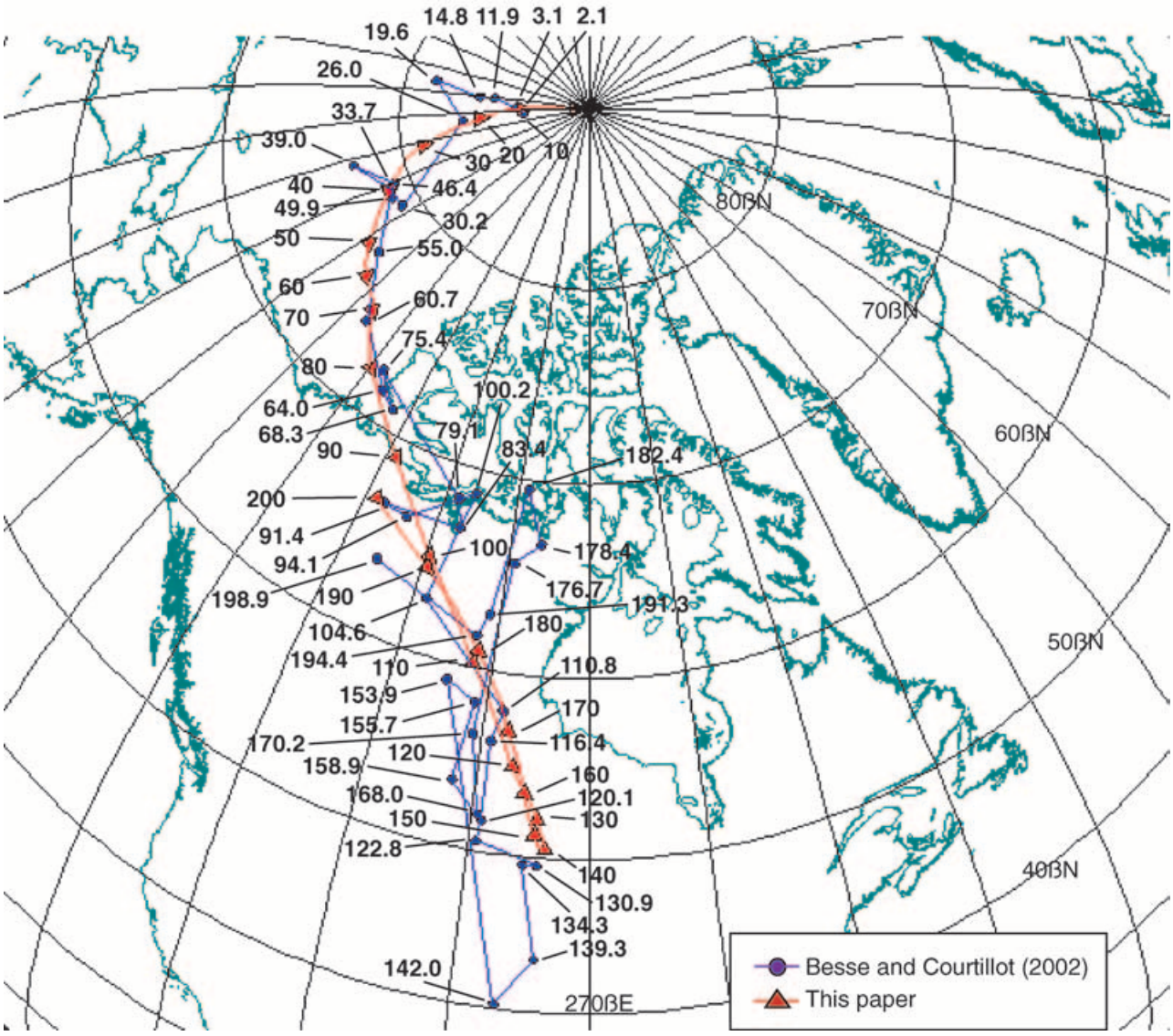

Figure 30. Comparison between the synthetic APW path for Central Africa proposed by Besse & Courtillot (2002) and the best-fit APW path calculated in this paper. Ages are in Ma.

Morgan, W.J., 1971. Convection plumes in the lower mantle, *Nature,* **230,** 42–43.

Morgan, W.J., 1983. Hot-spot tracks and the early rifting of the Atlantic, *Tectonophysics,* **94,** 123–139.

Müller, R.D., Royer, J.-Y. & Lawver, L.A., 1993. Revised plate motions relative to the hotspots from combined Atlantic and Indian Ocean hotspot tracks, *Geology,* **21**(3), 275–278.

Müller, R.D., Roest, W.R., Royer, J.-Y., Gahagan, L.M. & Sclater, J.G., 1997. Digital isochrons of the world's ocean floor, *J. geophys. Res.,* **102**(B2), 3211–3214.

Musgrave, R.J., 1989. A weighted least-squares fit of the Australian apparent polar wander path for the last 100 Myr, *Geophys. J,* **96,** 231–243.

O'Connor, J.M. & Duncan, R.A., 1990. Evolution of the Walvis Ridge—Rio Grande Rise hot spot system: implications for African and South American plate motions over plumes, *J geophys. Res.,* **95**(B11), 17 475–17 502.

Parker, R.L. & Denham, R., 1979. Interpolation of unit vectors, *Geophys. J. R. astr. Soc.,* **58,** 685–687.

Powell, C.M., Roots, S.R. & Veevers, J.J., 1988. Pre-breakup continental extension in East Gondwanaland and the early opening of the eastern Indian Ocean, *Tectonophysics,* **155,** 261–283.

Roeser, H.A., Fritsch, J. & Hinz, K., 1996. The development of the crust off Dronning Maud Land, East Antarctica, in *Weddel Sea Tectonics and Gondwana Break-up*, Geological Society Special Publication 108, pp. 243–264, eds Storey, B.C., King, E.C. & Livermore, R.A., The Geological Society, London.

Rowley, D.B. & Lottes, A.L., 1988. Plate-kinematic reconstructions of the North Atlantic and Arctic: Late Jurassic to Present, *Tectonophysics,* **155,** 73–120.

Royer, J.Y. & Chang, T., 1991. Evidence for relative motions between the Indian and Australian plates during the last 20 Myr from plate tectonic reconstructions: implications for the deformation of the Indo-Australian plate. *J. geophys. Res.,* **96,** 11 779–11 802.

Royer, J.-Y., Patriat, P., Bergh, H.W. & Scotese, C.R., 1988. Evolution of the Southwest Indian Ridge from the Late Cretaceous (anomaly 34) to the Middle Eocene (anomaly 20), *Tectonophysics,* **155,** 235–260.

Royer, J.Y., Müller, R.D., Gahagan, L.M., Lawver, L.A., Mayes, C.L., Nürnberg, D. & Sclater, J.G., 1992. *A Global Isochron Chart*, Technical Report 117, University of Texas Institute for Geophysics, Austin, TX.

Sahagian, D., 1988. Epeirogenic motions of Africa as inferred from Cretaceous shoreline deposits, *Tectonics,* **7**(1), 125–138.

Sandwell, D.T. & Smith, W.H.F., 1997. Marine gravity anomaly from Geosat and ERS 1 satellite altimetry, *J. geophys. Res.,* **102,** 10 039–10 054.

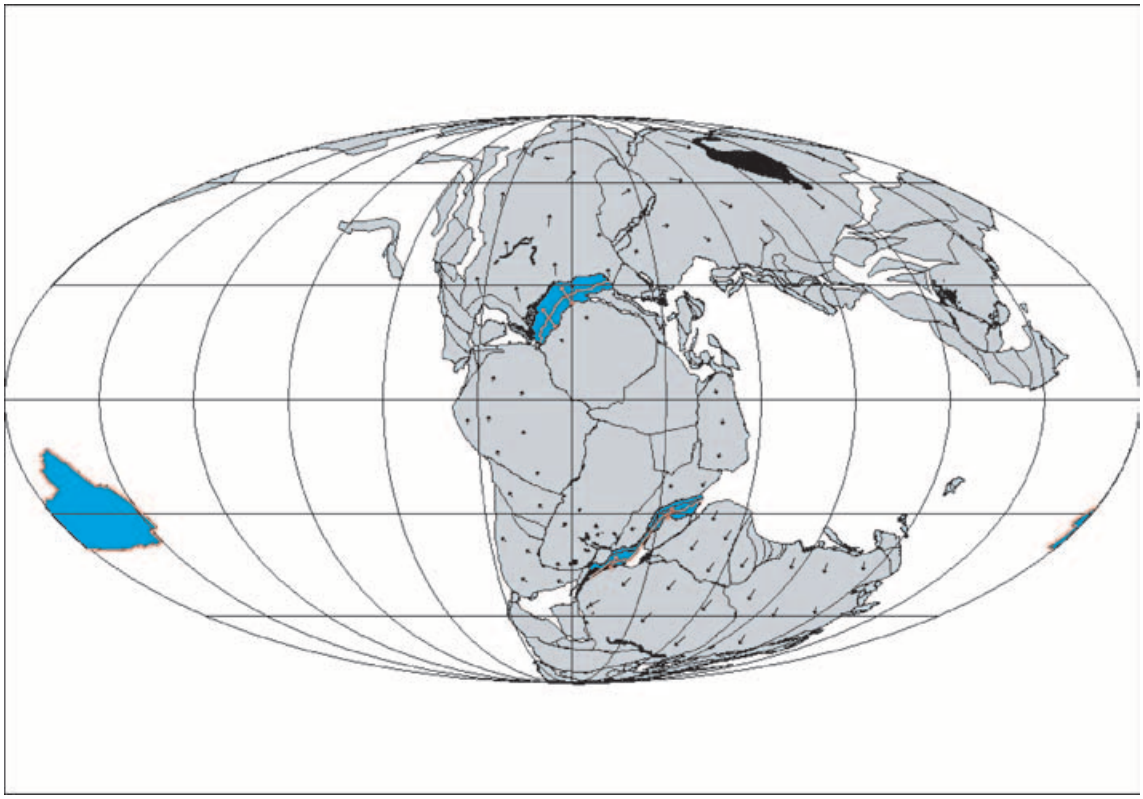

Figure 31. Reconstruction at chron M25 (154.3 Ma, Kimmeridgian). Arrows represent the direction and magnitude of the plate velocity field relative to the palaeomagnetic frame of reference. Double arrows represent the direction and rate of seafloor spreading. LIPS are shown in black, whereas blue areas represent those remnants of the oceanic crust that formed between ∼180 Ma and chron M25 and are still preserved in the present-day oceans.

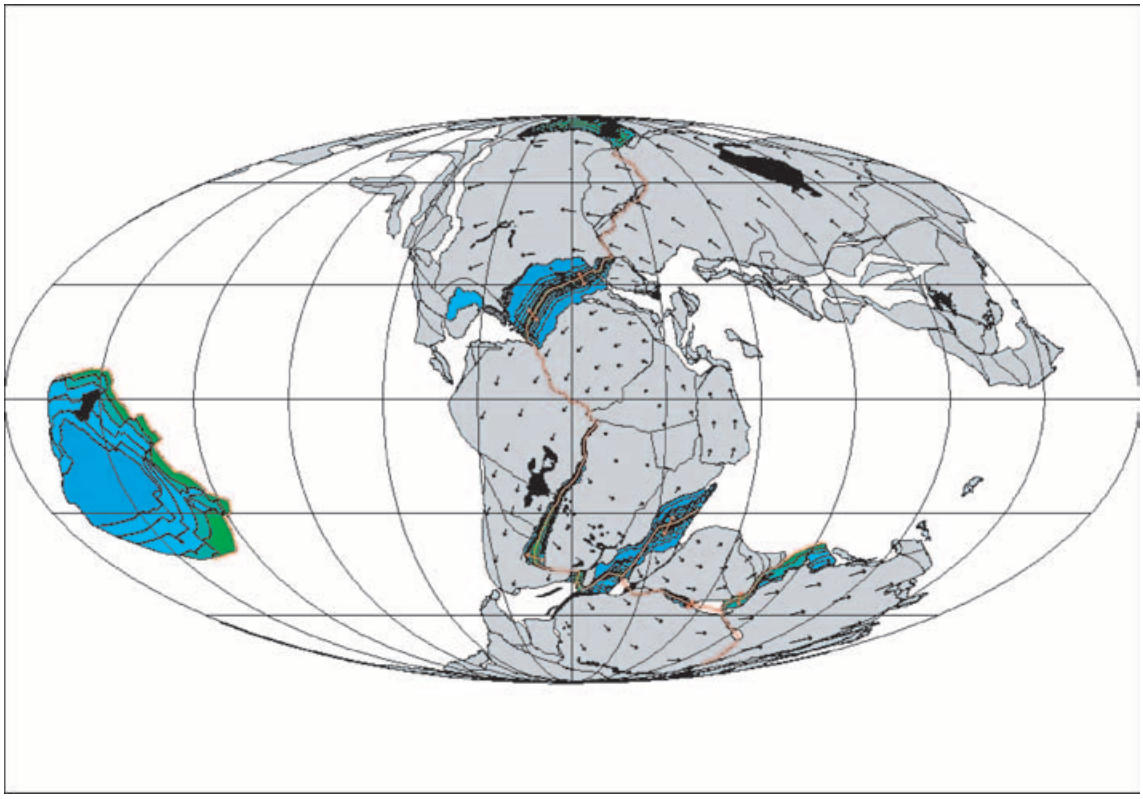

Figure 32. Reconstruction at chron M0 (120.4 Ma, Aptian). Arrows represent direction and magnitude of the plate velocity field relative to the palaeomagnetic frame of reference. Double arrows represent the direction and rate of seafloor spreading. LIPS are shown in black, spreading centres are in red. Colours in oceanic areas represent preserved oceanic crust bounded by isochrons M25, M21, M16, M10, M4 and M0.

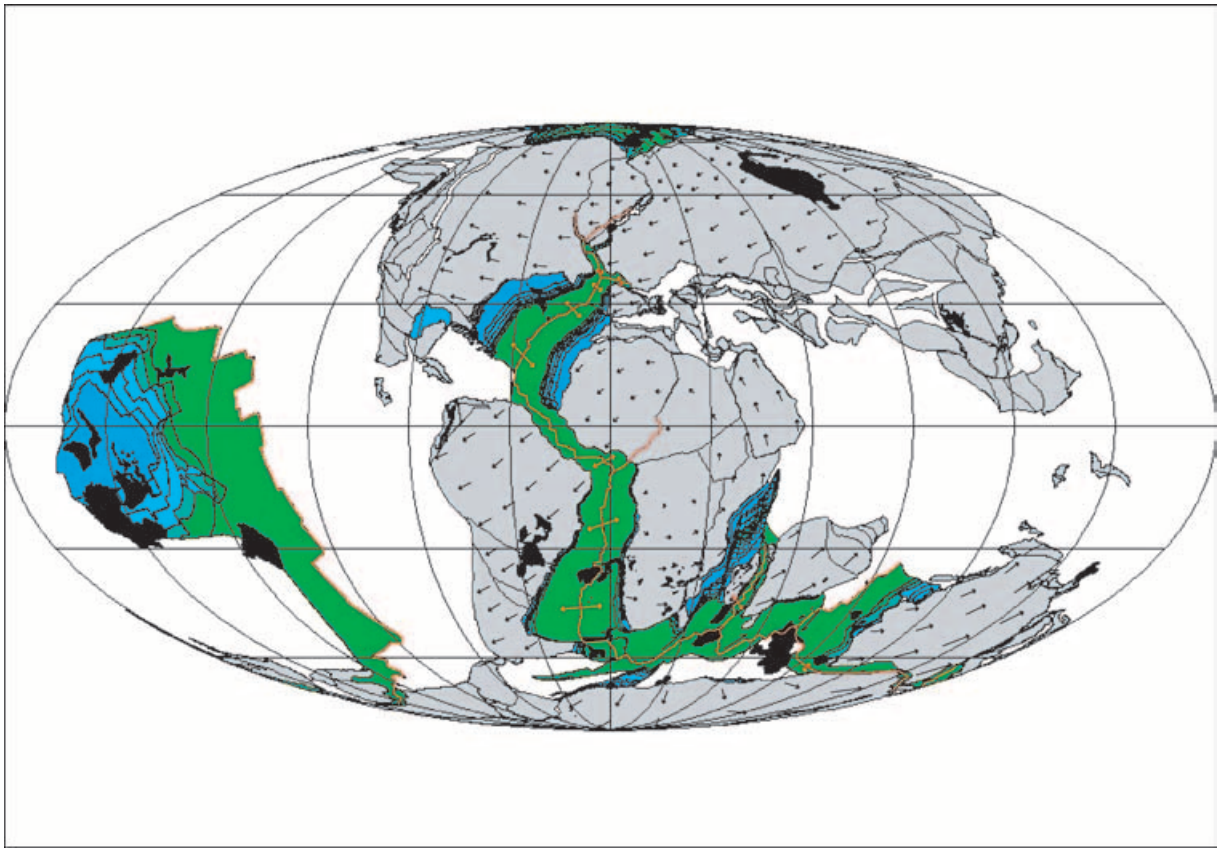

Figure 33. Reconstruction at chron C34 (83.5 Ma, Santonian–Campanian boundary). Arrows represent the direction and magnitude of the plate velocity field relative to the palaeomagnetic frame of reference. Double arrows represent the direction and rate of seafloor spreading. LIPS are shown in black, active spreading centres are in red. Colours in oceanic areas represent preserved oceanic crust bounded by isochrons M25, M21, M16, M10, M4, M0 and C34.

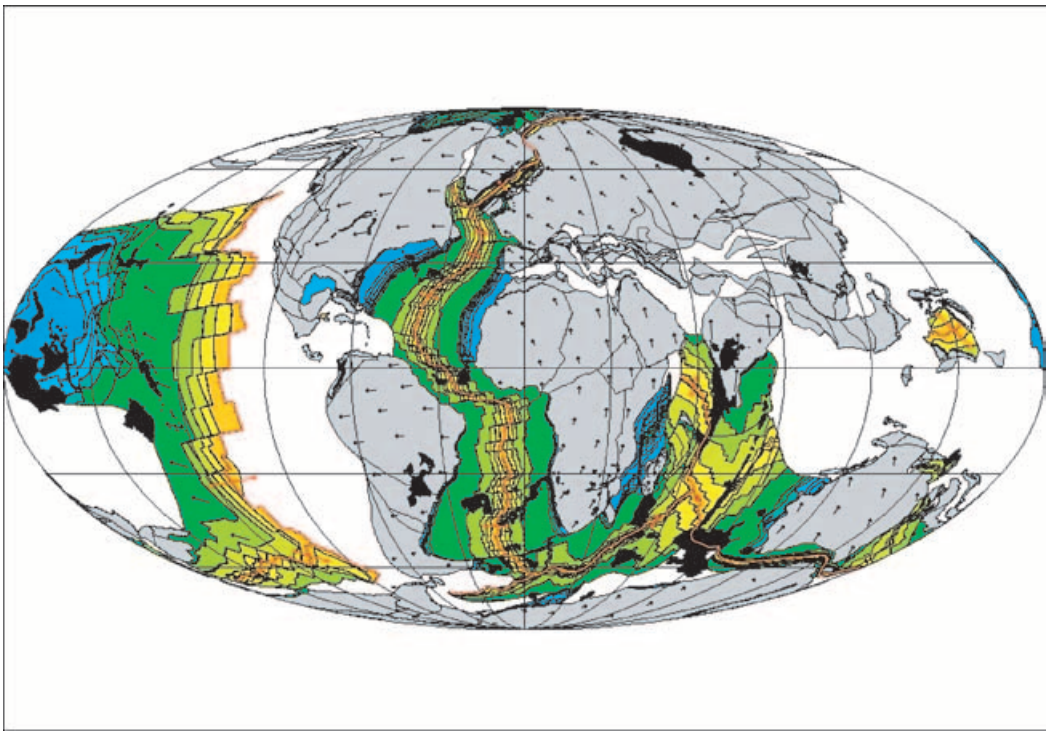

Figure 34. Reconstruction at chron C18 (40.1 Ma, Bartonian). Arrows represent the direction and magnitude of the plate velocity field relative to the palaeomagnetic frame of reference. Double arrows represent the direction and rate of seafloor spreading. LIPS are shown in black, active spreading centres are in red. Colours in oceanic areas represent preserved oceanic crust bounded by isochrons M25, M21, M16, M10, M4, M0, C34, C31, C25, C21 and C18.

Schettino, A., 1998. Computer aided paleogeographic reconstructions, *Comput. Geosci.,* **24**(3), 259–267.

Schettino, A., 1999. Polygon intersections in spherical topology: application to plate tectonics, *Comput. Geosci.,* **25**(1), 61–69.

Schettino, A. & Scotese, C.R., 2000. *A Synthetic APW Path for Africa (Jurassic-Present) and Global Plate Tectonic Reconstructions*, paper presented at the AGU Spring Meeting, Washington, May 30 to June 3.

Schettino, A. & Scotese, C.R., 2001. New internet software aids paleomagnetic analysis and plate tectonic reconstructions, *EOS, Trans. Am. geophys. Un.,* **82**(45), 530–536.

Schult, F.R. & Gordon, R.G., 1984. Root mean square velocities of the continents with respect to the hot spots since the Early Jurassic, *J. geophys. Res.,* **89**(B3), 1789–1800.

Scotese, C.R., 1990. *Atlas of Phanerozoic Plate Tectonic Reconstructions*, Paleomap Project Progress Report 01–1090, Department of Geology, University of Texas, Arlington, TX.

Scotese, C.R., Gahagan, L.M. & Larson, R.L., 1988. Plate tectonic reconstructions of the Cretaceous and Cenozoic ocean basins, *Tectonophysics,* **155,** 27–48.

Steinberger, B. & O'Connell, R.J., 1998. Advection of plumes in mantle flow: implications for hotspot motion, mantle viscosity and plume distribution, *Geophys. J. Int.,* **132,** 412–434.

Tarduno, J.A. & Cottrell, R.D., 1997. Paleomagnetic evidence for motion of the Hawaiian hotspot during formation of the Emperor seamounts, *Earth planet. Sci. Lett.,* **153,** 171–180.

Thompson, R. & Clark, R.M., 1981. Fitting polar wander paths, *Phys. Earth planet. Inter.,* **27,** 1–7.

Torsvik, T.H., Tucker, R.F., Ashwal, L.D., Carter, L.M., Jamtveit, B., Vidyadharan, K.T. & Venkataramana, P., 2000. Late Cretaceous India–Madagascar fit and timing of break-up related magmatism, *TerraNova,* **12,** 220–224.

Van der Voo, R., 1993. *Paleomagnetism of the Atlantic, Tethys and Iapetus Oceans*, Cambridge University Press, Cambridge.

Veevers, J.J., 1987. The conjugate continental margin of Antarctica and Australia, in *The Antartic Continental Margin: Geology and Geophysics of Offshore Wilkes Land*, pp. 45–74, eds Eittreim, S.L. & Hampton, M.A., Circum-Pacific Council for Energy and Mineral Resources Earth Science Series, 5A, Houston.

Wilson, M. & Guiraud, R., 1992. Magmatism and rifting in Western and Central Africa, from Late Jurassic to Recent times, *Tectonophysics,* **213,** 203–225.

Wilson, R.L., 1970. Permanent aspects of the Earth's non-dipole magnetic field over the Upper Tertiary times, *Geophys. J. R. astr. Soc,* **19,** 417–437.

Wilson, R.L., 1972. Palaeomagnetic differences between normal and reversed field sources, and the problem of far-sided and right-handed pole positions, *Geophys. J. R. astr. Soc,* **28,** 295–304.

Ziegler, A.M., Scotese, C.R. & Barrett, S.F., 1983. Mesozoic and Cenozoic paleogeographic maps, in *Tidal Friction and the Earth's Rotation II*, pp. 240–252, eds Brosche, P. & Sundermann, J., Springer-Verlag, Berlin.

SUPPLEMENTARY MATERIAL

The following supplementary material is available for this article online:

Figs 8–14 show analysis of residuals of regression for North America (Fig. 8), South America (Fig. 9), Eurasia (Fig. 10), India (Fig. 11), Central Africa (Fig. 12), Australia (Fig. 13) and Antarctica (Fig. 14).

Table 3 shows palaeopoles selected after the pre-filtering process and post-filtering flags.

Tables 5–11 show the results of the post-filtering process and spline regression analysis for North America (Table 5), South America (Table 6), Eurasia (Table 7), India (Table 8), Central Africa (Table 9), Australia (Table 10) and Antarctica (Table 11).

Table 13 shows synthetic palaeopoles rotated in Central African coordinates and best-fitting African APWP.

Table 14 shows the rotation model for Central Africa (200 Ma to present) in the palaeomagnetic reference frame.

This material is available as part of the online article from http://www.blackwell-synergy.com